PAPER

Check for updates

Per- and polyfluoroalkyl substances (PFAS) as environmental drivers of antimicrobial resistance: insights from genome sequences of *Klebsiella grimontii* and *Citrobacter braakii* isolated from contaminated soil†

Matteo Calcagnile, [ID] *[a] Andrea Giuliano, [ID] [bc] Maurizio Salvatore Tredici,[a] Davide Gualandris, [ID] [d] Davide Rotondo, [ID] [d] Antonio Calisi, [ID] [d] Chiara Leo, [ID] [e] Margherita Martelli, [ID] [e] Anna Rocchi, [ID] [e] Knud Erik Klint,[f] Francesco Dondero [ID] ‡[d] and Pietro Alifano [ID] ‡[a]

Per- and polyfluoroalkyl substances (PFAS) are man-made chemicals widely used for industrial applications since the 1940s. PFAS are extremely persistent in the environment, to the extent that they have earned the reputation of 'forever chemicals'. There is growing evidence that PFAS have a significant impact on the biodiversity, composition, and activity of microbial communities. In this study, we hypothesized that these compounds may increase the abundance of antibiotic-resistant bacteria. To investigate this hypothesis, we employed Winogradsky columns to study the microbial community's response to PFAS-contaminated soil from the Albäck fire drill site (Trelleborg, Sweden). Column amendment with a high amount of perfluorooctanoic acid (PFOA) led to selective growth, in the aqueous phase of the columns, of *Klebsiella grimontii* and *Citrobacter braakii*, two emerging opportunistic facultative anaerobic pathogens. Whole-genome sequencing of *K. grimontii* Tre-B and *C. braakii* Tre-T isolates revealed numerous antibiotic resistance genes (ARGs), with a notable prevalence of resistance to fluoroquinolones. Among these genes are those encoding multidrug efflux systems that confer resistance to a wide range of toxic compounds such as antibiotics, surfactants, dyes, detergents, and disinfectants. Both strains contain a large set of features involved in the degradation of aromatic and halogenated compounds, and other recalcitrant chemicals. *K. grimontii* Tre-B is characterized by the presence of an IncR-group plasmid (named pKGTreB) containing many genes involved in resistance to arsenic, copper, mercury, and silver. This strain also contains a choline utilization (cut) bacterial microcompartment (BMC) locus, which has been implicated in various human diseases as a source of trimethylamine (TMA). Understanding the genomes of these two bacterial strains provides insights into the molecular mechanisms responsible for their pathogenicity, antibiotic resistance, resistance to biocides, and heavy metal tolerance. In this study we also show that when the two bacteria were grown with PFOA, their resistance to certain aminoglycosides, fluoroquinolones and macrolides increased, and we found that transcript levels of the *kpnF*, *kpnG*, *adeF*, and *oqxA* antibiotic-resistance genes of *K. grimontii* Tre-B increased as a function of PFOA concentration, whereas *acrA* was upregulated only at low PFOA concentrations. These results indicate that PFOA, in addition to selecting specific groups of bacteria, may increase antibiotic resistance through upregulation of specific antibiotic resistance genes and suggest that these genes may also be involved in bacterial resistance to PFAS. Through the exploration of these mechanisms, we can gain valuable insights into how environmental pollutants, such as PFAS and other contaminants, may contribute to the development of antimicrobial resistance.

[a]Department of Experimental Medicine (DiMes), University of Salento, Lecce, 73100, Italy. E-mail: matteo.calcagnile@unisalento.it

[b]Department of Biological and Environmental Sciences and Technologies (DiSTeBA), University of Salento, Lecce, 73100, Italy

[c]Department of Medical Biotechnology, University of Siena, Siena, 53100, Italy

[d]Department of Science and Technological Innovation (DISIT), University of Eastern Piedmont "Amedeo Avogadro", Alessandria, 15121, Italy

[e]Polo d'Innovazione di Genomica Genetica e Biologia SRL, NGS & Bioinformatic Laboratory, 53100, Siena, Italy

[f]Geo, Maglebjergvej, 2800 Kgs. Lyngby, Copenhagen, Denmark

† Electronic supplementary information (ESI) available. See DOI: https://doi.org/10.1039/d4va00359d

‡ These authors contributed equally.

Paper |

Environmental significance

Per- and polyfluoroalkyl substances (PFAS), persistent environmental pollutants, disrupt soil microbial communities. PFAS accumulation in soil affects microbial diversity and function. Soil microorganisms play a crucial role in nutrient cycling, decomposition of organic matter, and maintaining overall soil stability. This study examined PFAS-contaminated soil using microcosms contaminated with perfluorooctanoic acid (PFOA) and identified *Klebsiella grimontii* Tre-B and *Citrobacter braakii* Tre-T as dominant bacteria. Both strains carried antibiotic resistance genes and virulence factors, suggesting PFAS contamination may promote the proliferation of potentially harmful, drug-resistant microbes. In addition, PFOA exposure causes an increase in the transcription levels of antibiotic-resistance genes of *K. grimontii* Tre-T and *C. braakii* Tre-B. This finding suggests a possible environmental mechanism by which PFAS can influence public health.

Introduction

Per and polyfluoroalkyl substances (PFAS) are man-made chemicals that comprise a large group of compounds that have an alkyl chain backbone, typically 4 to 16 carbon atoms in length, and a functional moiety (primarily carboxylate, sulfonate, or phosphonate).[1] The two most widely known PFAS contain an eight-carbon backbone, including perfluorooctanoic acid (PFOA) and perfluorooctane sulfonate (PFOS). PFAS, introduced in the latter half of the 20th century, have found extensive applications in hundreds of industrial and consumer products.[2] These applications span from water and stain-resistant coatings for textiles, leather, upholstery, and carpets to oil-resistant coatings for food-contact-approved paper. PFAS have also been used in various other industries, including chromium electroplating as mist suppressants, as surfactants in electronic etching baths, as photographic emulsifiers, in aviation hydraulic fluids, and in the manufacturing of paints, adhesives, waxes, polishes and fire-fighting foams.[3–5] The industrial success of PFAS, which resulted in an estimated annual production of thousands of tons at the turn of the century, can be attributed to their specific chemical and physical properties that make them ideal surfactants.[4] Additionally, the prevailing notion of these substances being biologically inert significantly contributed to their widespread use. However, recent studies have revealed that these compounds are extraordinarily persistent in the environment, earning them the moniker 'forever chemicals.' Furthermore, they have been shown to exert various biological effects, with adverse consequences for human health and ecosystems on a global scale.[4,6–15] For these reasons over the past decade, PFASs have been increasingly regulated. Currently, a few PFAS congeners and their salts or precursors are listed in the international Stockholm Convention under Annex A-elimination (PFHxS, PFOA) or B-restriction (PFOS), so their production and use is banned or restricted worldwide. In view of the regulations EU2020/784 and 2019/1021 in Europe PFOA should only be present in real life as a trace contaminant while the production and use of PFOS is still legal in a single industrial application, as a mist suppressant for non-decorative hard chrome plating (VI) in closed loop systems. C9-14 chain PFCA (and their related products) are restricted under REACH in the EU/EEA from February 2023. Despite these legal barriers, there are thousands of PFAS hotspots. 'The Forever Pollution Project' website (2023)[16] has estimated there to be approximately 17 000 confirmed sites globally in Europe, along with an additional 21 000 presumptive contamination sites resulting from current or past industrial activities. These sites are particularly prevalent around fluoropolymer plants but also military and drill sites as well as airports due to the extensive use of Aqueous Film Forming Foams (AFFFs) for fire extinguishing.

PFAS are generally resistant to microbial degradation,[17] and there is a growing body of evidence that PFOA and PFOS have a profound impact on the structure and function of microbial communities in diverse ecosystems.[18–24] On the other hand, there is little evidence on the real ability of microorganisms to effectively metabolize these compounds, although some models on the catabolism of these substances have been proposed.[15,25] PFAS contain high-energy carbon-fluorine bonds that occur very rarely in microbial chemistry and most importantly, the end-product of biodegradation, fluoride, can be very toxic to microorganisms.[26] Although some microbial metabolism with minimal PFAS degradation (defluorination) activity such as the anaerobic *Acidimicrobium* sp A6 strain, and Pseudomonades with bioaccumulation capabilities have been described (see Shahsavari *et al.*, 2021 (ref. 27)), information regarding the mode of action is scarce and bioremediation for environmental cleanup should not be deemed a practical option at present.[25] The impact of PFAS on the biodiversity, composition and activity of microbial communities has aroused particular concern. Indeed, the structure and correct functioning of microbial communities are crucial in the balance of biogeochemical cycles, pollutant decomposition, chemical transformation, food chain.[28–30] There is substantial evidence indicating that prolonged exposure to PFAS in soils, sediments, and vadose regions results in a marked reduction in biodiversity.[31,32] Additionally, this exposure tends to favor the enrichment of specific bacterial phyla, notably Proteobacteria, Acidobacteria, and Actinobacteria, which exhibit higher resistance to PFAS compared to other phyla.[18,22,33] This is possibly due to a different architecture of cell wall (*i.e.*, negatively-charged outer membrane in Proteobacteria), or a higher ability to cope with oxidative damage and/or DNA damage, or also an ability to extrude PFAS from the cells or immobilize these compounds in a biofilm.

Interestingly, experiments in microcosms have recently revealed that exposure to PFOA may significantly increase the abundance of antibiotic resistance genes (ARGs) and human bacterial pathogens (HBPs) raising further alarm for human health.[34] Studies conducted on conjugative strains of *E. coli* harboring the RP4 plasmid show that the spread of ARGs in PFAS-polluted environments may be due to the ability of PFASs to promote conjugative transfer of the ARG plasmid as a consequence of inducing oxidative stress, increasing cell

© 2025 The Author(s). Published by the Royal Society of Chemistry

Environ. Sci.: Adv., 2025, **4**, 1444–1476 | **1445**

membrane permeability, and stimulating excretion of extracellular polymeric substances that promote conjugative transfer.[35,36] PFAS have been also shown to increase transformation frequencies in *Acinetobacter baylyi*, a naturally competent bacterium commonly found in aquatic environment, thereby contributing to the spread of plasmid-borne antibiotic resistance genes.[37] Mechanistically, this increase in transformation frequencies was imputed to increased cell envelope permeability, biofilm formation, reactive oxygen species production, and upregulation of DNA uptake genes.[37] In addition, PFOA and PFOS have been shown to promote long-term plasmid stability and induce the expression of ARGs.[37]

The evidence that PFAS contamination may act as a driver for selection of environmental ARBs and promote the spread of ARGs is particularly worrisome as, in recent years, the spread of multidrug-resistant bacterial infections has raised global concerns.[38–40] The World Health Organization[41] (WHO, 2023) and the European Commission[42,43](EC, 2023) identified antimicrobial resistance (AMR) as a transboundary health threat – a One Health concern – encompassing human health, animal health, plant health, and environmental aspects, with impacts on food and nutrition security, economic development, and equity within societies.[44–46] The spread of AMR appears to be linked to factors associated with climate change and chemical contamination, as indicated by recent studies.[47–49] Therefore, it is imperative to gain a comprehensive understanding of the underlying mechanisms and drivers of antimicrobial resistance in order to effectively tackle it.

In this research, we present a comprehensive analysis of the whole genome sequences, obtained with a sequencing depth of $200\times$, along with pertinent traits and characteristics of two bacterial strains, namely *Klebsiella grimontii* and *Citrobacter braakii*. These strains were isolated from microcosm experiments prepared using soil samples obtained from the Albäck fire drill site in Trelleborg, Sweden, known for its residual contamination by PFAS congeners originating from heavy and light Aqueous Film-Forming Foams (AFFFs). This investigation provides insights into the genomic and functional attributes of these bacterial isolates, shedding light on their potential roles in the context of PFAS-contaminated environments. Characterized by abundance of antibiotic, surfactant, dye, detergent, disinfectant, and heavy metal resistance genes, *K. grimontii* and *C. braakii*, both opportunistic human pathogens, offer an avenue for future research. This exploration may shed light, even at a mechanistic level, on potential links between PFAS contamination and the global spread of bacterial and antibiotic resistance.

Materials and methods

Site characterization and sampling procedure of the Trelleborg site

The study area is the old Albäck landfill in Trelleborg, Sweden (Fig. 1). This former unlined domestic/industrial landfill has been utilized as a Fire Drill Site (FDS) for many years and has a significant history of Aqueous Film Forming Foam (AFFF) contamination in the underground water and soil.

Initially, 7 monitoring wells were drilled (B1–B7) for geological/chemical characterization. Soil and water sampling in and outside the firefighting site were completed in June 2022. In September 2022 a supplementary borehole B1B was drilled to 10 m depth immediately adjacent to the concrete floor that firefighters used as an exercise area and for washing tools from foam (Fig. 1). The drilling was performed using a hydraulic drill equipped with a 100 mm rotary steel auger, and a steel casing was installed during the drilling. Samples were described directly on the steel auger in 2 m sections. Then samples were collected for each 50 cm, carefully using steel tools cleaned with Ethanol between each sampling. The samples were stored in Rilsan plastic bags, which are diffusion-tight and PFAS-controlled by Eurofins, and kept cool in cooling boxes at 4 °C in the dark.

For the purposes of this study, the sample obtained at a depth of 7.5 m, consisting of the peaty organic soil, was selected for analysis. Upon completion of the drilling process, water from the subsurface aquifer was sampled using a sand filter and polypropylene plastic pipes.

After 16 hours, a newly installed submersible pump, equipped with a polypropylene plastic tube, was lowered into the well, and water was brought up to the surface for sampling purposes. All pumps and tubes have been tested for PFAS emission previously, and were accepted for sampling PFAS infested water samples.

Soil and water samples were placed in appropriate 100 mL containers made of polystyrene and high-density polyethylene (HDPE), respectively, certified as PFAS-free by the supplier Eurofins Laboratories Denmark. Subsequently, the samples were dispatched to the same laboratory for PFAS analysis.

PFAS analysis

PFAS analysis (sum of 17 congeners) in soil samples were carried out by means of LC-MS/MS according to DIN 38414-14. The following congeners were evaluated: PFBA (perfluorobutanoic acid), PFBS (perfluorobutane sulfonic acid), PFPeA (perfluoropentanoic acid), PFPeS (perfluoropentane sulfonic acid), PFHxA (perfluorohexanoic acid), PFHxS (perfluorohexane sulphonic acid), PFHpA (perfluoroheptanoic acid), PFHpS (perfluoroheptane sulfonic acid), PFOA (perfluorooctanoic acid), PFOS (perfluorooctane sulfonic acid), 6:2 FTS (fluorotelomer sulfonate), PFOSA (perfluorooctane sulfonamide), PFNA (perfluorononanoic acid), PFNS (perfluorononanesulfonic acid), PFDA (perfluorodecanoic acid), PFDS (perfluorodecanesulphonic acid), PFUnDA (perfluorodecanoic acid), PFUnDS (perfluorodecane sulphonic acid), PFDoDA (perfluorodecanoic acid), PFDoDS (perfluorodecane sulphonic acid), PFTrDA (perfluorotridecanoic acid), PFTrDS (perfluorotridecane sulphonic acid). Limit of detection was 0.1 ppb for all congeners except PFOA and PFOS, 0.05 ppb; PFNS, 0.2 ppb; PFUnDS, PFDoDS, PFTrDS, 1 ppb. Determination of dry residue and water content was carried out according by means of thermogravimetric analysis according to the Swedish standard SS-EN 12880.

PFAS analysis (sum of 22 congeners) in water samples were carried out by means of LC-MS/MS according to DIN38407-42.
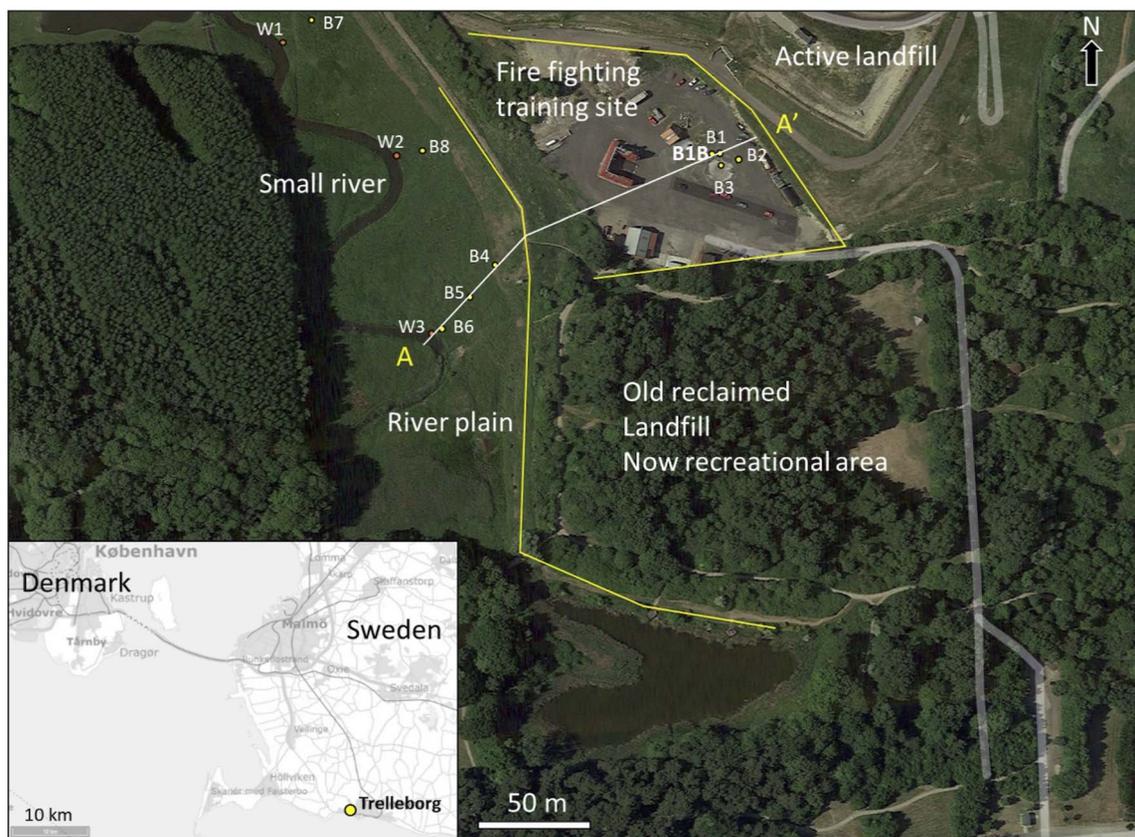
Fig. 1 Location of the Trelleborg site and position of the monitoring wells B1–B7 and B1B (Fig. 2) and existing wells, W1–W3. Cross section A–A′ was constructed for visualizing the geological settings on the site (Fig. 3).

PFBA (perfluorobutanoic acid), PFBS (perfluorobutane sulfonic acid), PFPeA (perfluoropentanoic acid), PFPeS (perfluoropentane sulfonic acid), PFHxA (perfluorohexanoic acid), PFHxS (perfluorohexane sulphonic acid), PFHpA (perfluoroheptanoic acid), PFHpS (perfluoroheptane sulfonic acid), PFOA (perfluorooctanoic acid), PFOS (perfluorooctane sulfonic acid), 6:2 FTS (fluorotelomer sulfonate), PFOSA (perfluorooctane sulfonamide), PFNA (perfluorononanoic acid), PFNS (perfluorononanesulfonic acid), PFDA (perfluorodecanoic acid), PFDS (perfluorodecanesulphonic acid), PFUnDA (perfluorodecanoic acid), PFUnDS (perfluorodecane sulphonic acid), PFDoDA (perfluorodecanoic acid), PFDoDS (perfluorodecane sulphonic acid), PFTrDA (perfluorotridecanoic acid), PFTrDS (perfluorotridecane sulphonic acid). Limit of detection was 0.3 ppt for all congeners except PFOS, 0.2 ppt; PFBA, 0.6 ppt; PFUnDS, PFDoDS, PFTrDS, 1 ppt.

Installation of Winogradsky columns and microbial isolation

Two sets of Winogradsky columns (microcosms) were set up using soil sampled 7.5 m deep at the PFAS-contaminated Trelleborg site B1 (Fig. 1). The columns were structured, from top to bottom, in: (i) an aqueous phase consisting of 25 mL of PFAS contaminated groundwater taken from the same site described above; (ii) a first layer of 50 mL consisting of 50 g of soil ("top layer"); (iii) a second layer of 50 mL consisting of 50 g of soil, 0.25 g of $CaCO_3$, 0.5 g of Na_2SO_4 and 1 g of soy flour ("bottom layer"). In one set of columns (PFOA columns), 5 mL of 40 mg per mL PFOA in 50% isopropanol (VWR, Radnor, Pennsylvania, USA) (final concentration of PFOA: 2 mg mL^{-1}; final concentration isopropanol: 2.5%) was added to the upper and lower layers. In the second set of columns (CTL columns), 5 mL of 50% isopropanol was added as control. The columns were incubated for 2 months at room temperature, then serial dilutions of the aqueous phase were plated onto LB agar medium [NaCl 10 g, tryptone 10 g (BD Difco™ Bacto™, Franklin Lakes, New Jersey, USA), yeast extract 5 g (BD Difco™ Bacto™, Franklin Lakes, New Jersey, USA), agar 15 g (BD Difco™ Bacto™, Franklin Lakes, New Jersey, USA), distilled water up to 1 L] containing 2 mg per mL PFOA (stock solution: of 40 mg per mL PFOA in 50% isopropanol) and incubated for 48 h at 28 °C. A workflow of the sampling and analysis processes carried out on the microcosms is provided in Fig. S1.† Unless otherwise specified, the reagents were sourced from Sigma-Aldrich (Merck, Darmstadt, Germany).

DNA extraction from bacterial isolates

The DNA was extracted as previously reported.[50] Briefly, bacterial isolates were grown in 250 mL flasks containing 50 mL LB broth. The flasks were incubated at 37 °C and 180 rpm. When the absorbance at 600 nm of the culture broth was 0.6, the growth was stopped by incubating the cultures on ice. The bacteria were collected using a centrifuge (Eppendorf,

© 2025 The Author(s). Published by the Royal Society of Chemistry

Environ. Sci.: Adv., 2025, **4**, 1444–1476 | **1447**

Hamburg, Germany) at 4000 rpm, 4 °C, and 30 min, and frozen for 24 h. The pellet was resuspended in SET Buffer [75 mM NaCl, 25 mM EDTA, 20 mM Tris–HCl pH 7.5], lysozyme was added to a final concentration of 1 mg mL^{-1} (w/v) and the samples were incubated for 60 min at 37 °C. After this time, proteinase K at a concentration of 0.5 mg mL^{-1} (w/v) and SDS (VWR, Radnor, Pennsylvania, USA) at 1% (v/v) were added. Samples were incubated at 55 °C for 60 min. Total nucleic acids were extracted by phenol : chloroform : isoamylic alcohol (25 : 24 : 1 [v/v/v]) and RNase A (final concentration 15 μg mL^{-1} (w/v)) was used to remove RNA (15 min at 37 °C). The nucleic acid extraction procedure was repeated to eliminate RNase A. The DNA was precipitated by adding cold ethanol and Na-acetate pH 7.3 M and incubating the samples at −20 °C overnight. A centrifuge was carried out to collect the pellet (10.000 rpm, 15 min, 4 °C), which was then washed with 80% ethanol, left to dry at room temperature, and resuspended in 100 μL of sterile water. The quality and the concentration of DNA samples were assessed by electrophoresis analysis and UV-spectrophotometry (NanoDrop®, ND-1000 Spectrophotometer, Thermo Fisher Scientific, Waltham, Massachusetts, USA). Unless otherwise specified, the reagents were sourced from Sigma-Aldrich (Merck, Darmstadt, Germany).

Screening of bacterial isolates by repetitive extragenic palindromic sequence-based PCR (rep-PCR)

PFOA-resistant colonies were characterized at the molecular level using the repetitive extragenic palindromic sequences-based polymerase chain reaction (REP-PCR) method.[50] The DNA was extracted as previously reported and used as a template to amplify the REP sequence using the BoxA1-R primer (5′-CTACGGCAAGGCGACGCTGACG-3′). The PCR reaction was implemented using 1 μL of template DNA, 1.25 μL of BoxA1-R primer, 2.5 μL of 10× buffer S (VWR, Radnor, Pennsylvania, USA), 2.5 μL of DMSO, 0.5 μL Taq DNA polymerase (VWR, Radnor, Pennsylvania, USA) and sterile water to a final volume of 25 μL. The PCR cycles used were the following: (1) initial denaturation (95 °C, 7 min); (2) denaturation (95 °C, 1 min); (3) annealing (52 °C, 1 min); (4) extension (65 °C, 8 min); (5) final extension (65 °C, 16 min). Steps 2, 3, and 4 were repeated 30 times. The amplicons were analyzed by electrophoresis analysis (1% (w/v) agarose gel, 75 eV, 1× TBE buffer). The electrophoresis gel image was acquired using the Chem-iDoc Imaging System (BIO-RAD, Hercules, California, USA). Unless otherwise specified, the reagents were sourced from Sigma-Aldrich (Merck, Darmstadt, Germany).

Minimum inhibitory concentration (MIC) and minimum bactericidal concentration (MBC) tests

Minimum inhibitory concentration (MIC) experiments were performed as previously described.[51] E. coli strain FB8 was used as a reference strain. This is an E. coli reference strain, also known as GC2553, K12S (Luria) or UTH1038, deposited at the University of Texas/Houston stock culture collection, genotype F-l-/lS, ftsR1, and is a prototrophic strain.[52–54] The MIC of ampicillin, metals, and PFOA were determined using 24-well plates and LB broth.

Briefly, the wells of the multiwell plates (CytoOne®, Milan Italy) were filled with 1 mL of LB broth inoculated with bacterial isolates (one colony in 10 mL of LB broth). 2 mL of inoculated broth was added to the first well. One volume of the molecule to be tested was added to the first well so that the final concentration was 500 μg mL^{-1} (w/v) for ampicillin; 100 mM for chromium (Cr), aluminum (Al), cobalt (Co), nickel (Ni), copper (Cu) zinc (Zn) and 320 mM for silver (Ag). Subsequently, serial dilutions 1 to 2 were carried out. For the metals Cr, Al, Co, Ni, Cu, and Zn 10 dilutions were carried out (from 100 mM to 0.2 mM). For ampicillin, 11 dilutions were carried out (from 500 μg mL^{-1} to 0.5 μg mL^{-1}). E. coli ATCC 25922 (NCTC 12241, CIP 76.24, DSM 1103, CCUG 17620, CECT 434), an Eucast routine quality control strain, was used to assess the accuracy and reliability of antibiotic susceptibility testing. For silver, 14 dilutions were carried out (from 320 mM to 0.04 mM). The compounds used to perform the MICs of the metals were the following: KCr(SO$_4$)$_2$·12H$_2$O, Al$_2$(SO$_4$)$_3$·8H$_2$O, CoCl$_2$·6H$_2$O, NiCl$_2$·6H$_2$O, CuCl$_2$·2H$_2$O, ZnCl$_2$, AgNO$_3$. The MIC for fluoride was performed similarly to the previous ones and sodium fluoride (NaF) was used. The NaF powder was solubilized in LB at a concentration of 1 M. 2 mL of this solution was used to fill the 1st well. Subsequently, serial 1 to 2 dilutions were made using LB as a diluent. The MIC for PFOA was performed by filling 10 wells of the multiwell plate with inoculated LB broth and adding a volume of PFOA solution so that the final concentration of the compound in the wells was: 10 mg mL^{-1} for the 1st well, 9 mg mL^{-1} for second well, 8 mg mL^{-1} for third well, 7 mg mL^{-1} for fourth well, 6 mg mL^{-1} for fifth well, 5 mg mL^{-1} for sixth well, 4 mg mL^{-1} for seventh well, 3 mg mL^{-1} for the eighth well, 2 mg mL^{-1} for the ninth well, and 1 mg mL^{-1} for the tenth well. The PFOA stock solution used in this experiment had a concentration of 200 mg mL^{-1} (w/v). PFOA was solubilized in a mixture of 50% isopropyl alcohol in water. To control and normalize the MIC data, the solubilization solution (50% isopropyl alcohol in water) was used to set up a MIC experiment without the PFOA. In each MIC experiment setup, one well containing only LB (positive control) was foreseen. The experiments were repeated three times. In addition, the minimal bactericidal concentration (MBC) was measured after the MIC. For each experiment, a 100 μL aliquot was taken from each well and washed 2 times with sterile LB. The samples were centrifuged (3000 rpm, 5 min) to collect the pellet. The pellet obtained after the washings was resuspended in 100 μL of sterile LB, and 10 μL of suspension was plated on LB agar. The plates obtained in this way were incubated at 37 °C. After 24 h, growth was observed. The MBC was considered the lowest concentration of substance for which no growth was observed. Unless otherwise specified, the reagents were sourced from Sigma-Aldrich (Merck, Darmstadt, Germany).

Antimicrobial susceptibility of C. braakii Tre-T and K. grimontii Tre-B in the presence of PFOA

The antimicrobial susceptibility of C. braakii Tre-T and K. grimontii Tre-B was assessed by the Kirby–Bauer method following the guidelines established by EUCAST v.15 (2025). Bacterial strains were grown on Mueller–Hinton agar plates (BD Difco™ Bacto™, Franklin Lakes, New Jersey, USA) supplemented with an

isopropanol-PFOA solution (final concentration of PFOA of 2 μg mL^{-1}, 20 μg mL^{-1}, 200 μg mL^{-1}, 2 mg mL^{-1}) or isopropanol as a control. The inoculum was standardized to approximately 1.5×10^8 CFU mL^{-1}. Sterile swabs were used to inoculate the surface of the agar plates with each bacterial suspension. Then, antibiotic disks (Liofilchem, Roseto degli Abruzzi, Italy) were placed onto the agar surface using sterile forceps. Plates were incubated at 37 ± 1 °C for 18 hours. This method was used to determine the susceptibility to the following antibiotics: ampicillin 10 μg (AMP10), cefoperazone 30 μg (CAZ30), ceftazidime 30 μg (CFP30), amikacin 30 μg (AK30), tobramycin 10 μg (TOB10), pefloxacin 5 μg (PEF5), pipemidic acid 20 μg (PI20), azithromycin 15 μg (AZM15), tetracycline 30 μg (TE30), and trimethoprim-sulfamethoxazol 25 μg (SXT25). The quality of the antibiotic disks and agar plates was assessed using *E. coli* ATCC 25922. Unless otherwise specified, the reagents were sourced from Sigma-Aldrich (Merck, Darmstadt, Germany).

Antibiotic resistance gene transcription levels in the presence of PFOA (RT-qPCR)

K. grimontii Tre-B was grown in LB broth supplemented with PFOA to measure the impact of PFOA on the transcription levels of the antibiotic resistance genes. Briefly, *K. grimontii* Tre-B was inoculated in 10 mL of LB broth and the culture was incubated at 37 °C and 180 rpm for 18 h. Then, 50 mL flasks were inoculated 1 : 100 and incubated under the same conditions for 5 h, when the bacterial culture reached an OD$_{600nm}$ of 0.6. These flasks contained 10 mL of LB broth supplemented with an isopropanol–PFOA solution (final concentration of PFOA of 2 μg mL^{-1}, 20 μg mL^{-1}, 200 μg mL^{-1}) or isopropanol as a control. After the growth, bacterial cultures were centrifuged at 10 000 rpm for 1 minute, and then the supernatant was discarded. The RNA was extracted using the Aurum™ Total RNA Mini Kit according to the manufacturer's instructions and the extracts were quantified using UV spectrophotometry (NanoDrop®, ND-1000 spectro-photometer). Reverse transcription and qPCR reactions were performed using protocols, reagents, and instruments previously described.[55] All the experiments were repeated three times. The primers used for this analysis were: *acrA*_F (5′-GCGCTAACAGGATGTGACGAC-3′) and *acrA*_R (5′-ACCTGAGGACGAACTTCCGC-3′), *adeF*_F (5′-ATCACCGGAT-TAATCGCCATC-3′) and *adeF*_R (5′-CAGCGACGGATTTCATG-TAC-3′); *oqxA*_F (5′-TACTCTCCGCGCTCCTCGTC-3′) and *oqxA*_R (5′-CTCCTGACCGTCGGTGTAATTC-3′); *kpnF*_F (5′-GCTGGCGCTGGCTATCGCGC-3′) and *kpnF*_R (5′-GGCAATGGTCGCCGCGATGC-3′); *kpnG*_F (5′-GCGTCACTTC-GAAGAGACCG-3′) and *kpnG*_R (5′-GTCTGGTCGAGGGTGAC-CAG-3′); and *rpoB*_F (5′-ATGGTTTACTCCTATACCGAG-3′) and *rpoB*_R (5′-CCTGAAGGGCAGTATGGTCTGG′). Unless otherwise specified, the reagents were sourced from BIO-RAD (Hercules, California, USA). Statistical significance of the results was calculated using Student's *t*-test.

16S rRNA metabarcoding

The aqueous phases and the layer of surface soil soaked in water were collected from microcosms biostimulated or not with PFOA (Fig. S1†). The water and soil mixtures were used to extract DNA using the E.Z.N.A.® Soil DNA Kit (Omega Bio Tek, Norcross, GA, USA). The quality and concentration of the extracts were measured using Nanodrop® (ND-1000 spectro-photometer). The amplification, sequencing (Illumina MiSeq, San Diego, California, USA), and taxonomic assignment process were performed as previously described.[56] The Greengenes database (gg_13_5) (**https://greengenes.lbl.gov/**) was used for taxonomic assignment.[57]

Whole genome sequencing: preparation of DNA libraries and Illumina sequencing

Bacterial strains were cultured in 250 mL flasks containing 50 mL of LB broth. The flasks were incubated at 37 °C and 180 rpm. The growth of the bacteria was measured by monitoring the absorbance at 600 nm (V-10 PLUS spectrophotometer, ONDA). When the absorbance reached a value of 0.6, bacterial growth was stopped by incubating the flasks on ice. DNA extraction was performed as previously described. The DNA libraries were prepared according to the Illumina DNA Prep kit following the manufacturer's instructions (Illumina, San Diego, California, USA). Their quality was checked using the Fragment Analyzer™ High Sensitivity Small Fragment (Agilent Technologies, Santa Clara, California, USA) and Qubit® 4.0 Fluorometer (Thermo Fisher Scientific, Waltham, Massachusetts, USA). Finally, the libraries were loaded onto an Illumina MiSeq platform and sequenced with 2×150 bp paired-end run and V2 chemistry at the Polo GGB sequencing facility (Polo d'Innovazione di Genomica, Genetica e Biologia, Siena, Italy).

De novo genome assembly

The quality of the demultiplexed samples was checked using the program FastQC v0.11.9.[58] The reads were then *de novo* assembled using the assembler MaSuRCA v5.0.2.[59] The completeness and contiguity of the final assembly was evaluated using BUSCO (v5.2.2, with database bacteria_odb10)[60] based on the evolutionarily informed expectations of gene content from near-universal single-copy orthologs. The quality of the assembly was assessed using the program QUAST 5.0.2.[61]

Genomic data analysis

The tools Prokka v 1.14.6 (ref. 62) and DFAST v1.2.18 (ref. 63) were applied to identify main features of the sample genomes, including architecture, composition and functions. The taxonomic identification was performed using the program DFAST_QC[63] using as a comparison the Genome Taxonomy Database (GTDB).

The program Resistance Gene Identifier v6.0.3 (ref. 64) was used to identify resistance genes by comparing the assembled genomes to the Comprehensive Antibiotic Resistance Database (CARD). The tools PathogenFinder[65,66] and VirulenceFinder-2.0 (ref. 67) were further used to detect other virulence factors along the assembled Tre-B and Tre-T genomes. The online tool AntiSMASH 7.0 (ref. 68) was used to identify clusters containing genes involved in the secondary metabolism. Finally, the presence of mobile genetic elements in the genomes was analyzed using the MobileElementFinder tool.[69]

© 2025 The Author(s). Published by the Royal Society of Chemistry

Environ. Sci.: Adv., 2025, **4**, 1444–1476 | **1449**

Co-occurrence and genome neighborhood analysis

The Enzymatic Similarity Tool (EFI-EST) was used to calculate the co-occurrence of genes close to the *cutC* (OKNGJBID_00805), *eutB* (OKNGJBID_01616) and *pduE* (OKNGJBID_04294) genes of *K. grimontii* Tre-B and the *eutB* (LBFIJIGF_02983) and *pduE* (LBFIJIGF_03409) genes of *C. braakii* Tre-T.[70,71] Initially using the protein sequences as input, a sequence similarity network (SSN) was generated (option A: Blast), with an alignment score cutoff of 20. The resulting full network was submitted to EFI-GNT to generate a Genome Neighborhood Networks (GNNs) useful to analyze the co-occurrence and neighboring of Pfam families.[70,71] This tool also produces Genome Neighborhood Diagrams (GNDs) which have been used to visualize conserved genes.[70,71] SSN and GNN were analyzed with Cytoscape (v 3.10.0).[72] The composition of the generated datasets was manually analyzed to identify the most numerous bacterial genera showing conservation in the genomic region under analysis. EFI-EST and EFI-GNT analysis was also performed using the putative fluoride ion transporter (*crcB*) gene of both bacterial isolates: *K. grimontii* Tre-B (OKNGJBID_03358) and *C. braakii* Tre-T (LBFIJIGF_01727). The genes from *cut*, *eut* and *pdu* loci were also used to confirm the annotation using BLAST and as reference the *Salmonella enterica* subsp. *enterica* serovar Typhimurium str. LT2 (NCBI reference sequence: NC_003197.2) and *Escherichia coli* 536 complete sequences (NCBI reference sequence: NC_008253.1). The spread and conservation of the locus *cut* in *K. grimontii* specie were analyzed manually using the NCBI nucleotide database. Gene maps were drawn using Illustrator for Biological Sequences 2.0.[73]

Results

Geological setting of the Trelleborg site and analysis of PFAS

A sampling campaign was conducted at the firefighting site situated near the old Albäck landfill in Sweden, which serves as one of the demonstration units within the European project SCENARIOS (https://scenarios-project.eu) aimed at assessing the impact of PFAS congeners on the environment. Central to our inquiry is the detailed depiction presented in Fig. 1, where borehole B1 is positioned strategically directly above the elevated exercise area, which has been exposed for decades to 3 M light water AFFF containing PFOS and other PFAS precursors. This firefighting foam is specifically designed for combating hydrocarbon and polar solvent fuel fires. Various samples were obtained from depths ranging from 0 m to 9 m.

Based on the descriptions, a lithological log was constructed (Fig. 2). The log indicates that the upper 1.0 m consists of a sandy matrix with a dark brown fill containing large amounts of plastic waste. From 1.0 m onwards, the soil becomes richer in clay, and by 1.5 m, waste makes up more than 50% of the volume, with the fill primarily consisting of plastic, concrete, glass, and wood. At a depth of 4.0 m, the waste becomes sandier, with remnants of tires, rock wool, and even more wood, plastic, and glass. For these reasons, it is important to consider that there may be interactions between PFAS and co-contaminants.

It has been demonstrated that certain contaminants, such as microplastics, can serve as long-range transport media for PFAS.[74,75] Additionally, organic solvents can impede the chemical transformation of PFAS,[76] while heavy metals promote their adsorption into the soil.[77] At 6.8 m below ground surface (b.g.s.), the drill reaches the groundwater table, and at 7.0 m, the waste layer ends. Here, the natural soil begins, consisting of approximately 70 cm of dark brown organic peat. Beneath this peat layer, there is a 20 cm thick layer of laminated freshwater clay, poor in calcium carbonate ($CaCO_3$), containing strings of silt and fine sand. At 7.9 m b.g.s., a nearly 2 m thick layer of fine to medium grey meltwater sand, rich in $CaCO_3$, appears. Finally, from 9.7 m to the bottom at 10 m b.g.s., the drill encounters sandy, gravelly clay till. This till is grey, indicating reduced conditions, and firm, classified as basal clay till deposited under a transgressing glacier during the last stage of the Weichselian glaciation, around 13 000 BP. In Fig. 3, a cross-section from the Albäck River to the firefighting facility at well B1B is presented. The cross-section reveals that the area consists of a 55-million-year-old Danien limestone basement, located between 7 and 4 meters below the reference elevation, according to the Danish Vertical Reference 1990 (DVR 90). During glacial times, glaciers eroded the limestone, and basal clay till was deposited directly on top of it. After the glacier's retreat, a meltwater river eroded the clay till and deposited meltwater sand in an ancient riverbed. In the post-glacial period (less than 11 000 BP), freshwater sand and clay were deposited on top of the meltwater sediments in the riverbed. Over time, vegetation accumulated in this meandering river system, forming layers of peat, clay, and sand. In modern times, human activities have led to waste being deposited in parts of this old river system. Eventually, parts of the waste deposit site were reclaimed, and a firefighting facility was constructed on top of the former landfill. It may be concluded that the meltwater sand is hydraulically well connected throughout the area and that the freshwatersand is following channels in a classic meander riversystem with creation of oxbowlakes and lagunes with freshwaterclay/laminated silt/fine sand, that grows into peat bogs. Accordingly the infiltrating land fill percolate may potentially spread to the Albäck River downgradient to the west and south.

Table 1 displays the results of chemical analyses, detailing the concentrations of PFAS observed at the 7.5 m sampling height of borehole B1. Despite the concentration of PFAS found in this specific layer was not particularly high, *i.e.* sum of PFAS (17 congeners, see Materials and methods) 56.97 ppb, this depth harbors a rich, dark-brown organic peat layer located directly beneath the water table, where percolates from the upper strata accumulate. Below this organic layer, the borehole's geological composition comprises laminated clay with silt interspersed with sand stringers, which serves to support the peat layer. Notably, this clay layer, primarily composed of impermeable clay, is instrumental in accumulating PFAS present in leachate or groundwater due to its impermeability. Additionally, the distinct layer features grey meltwater sand and exhibits a low concentration of calcium carbonate ($CaCO_3$).
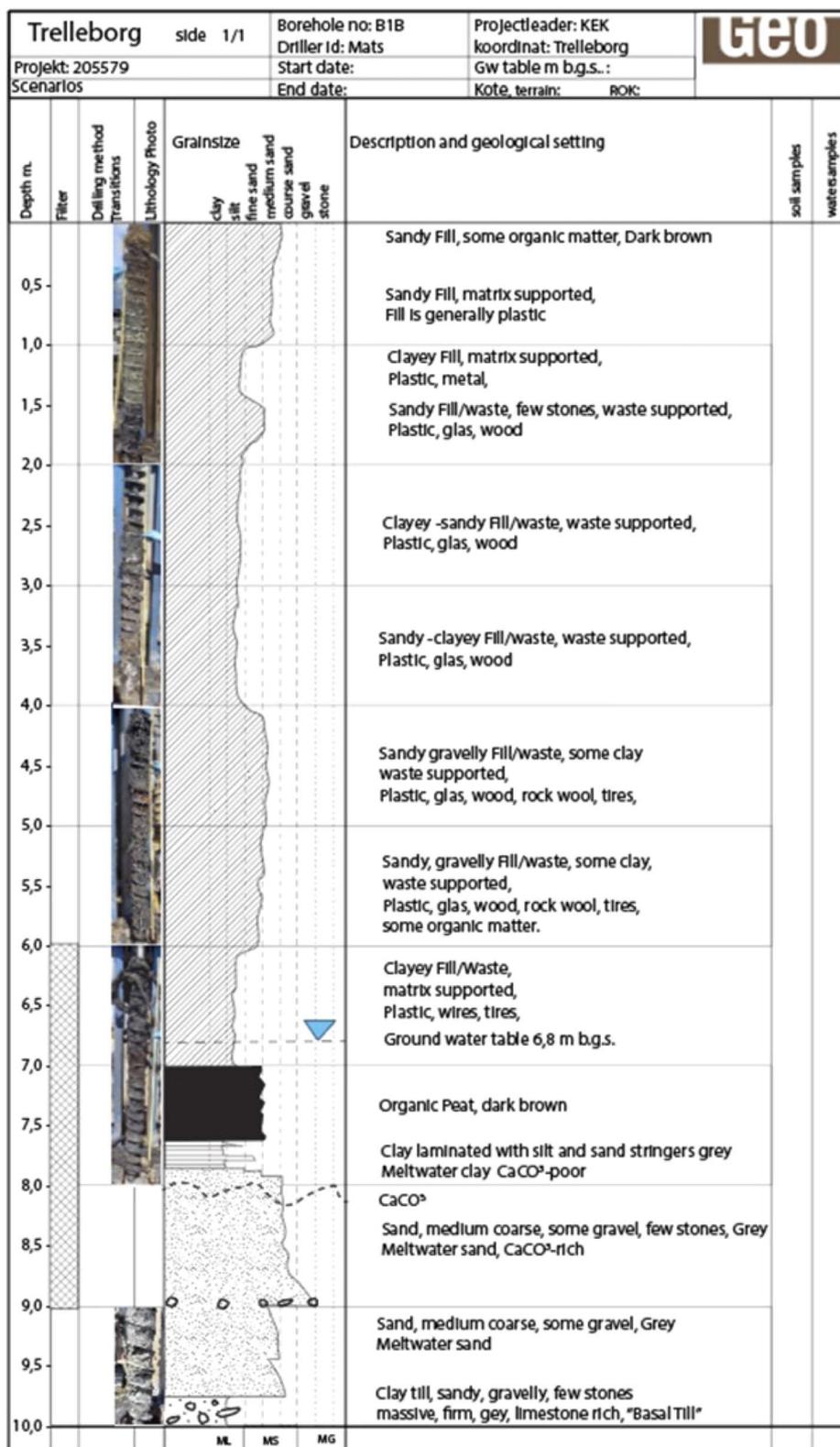
Fig. 2   Lithological log from well B1B. The log exhibits a detailed description of the soil samples collected including grain-size distribution and textural properties of the samples. Specific samples for this study were collected from the 70 cm thick peat layer between 7 and 7.7 m b.g.s.
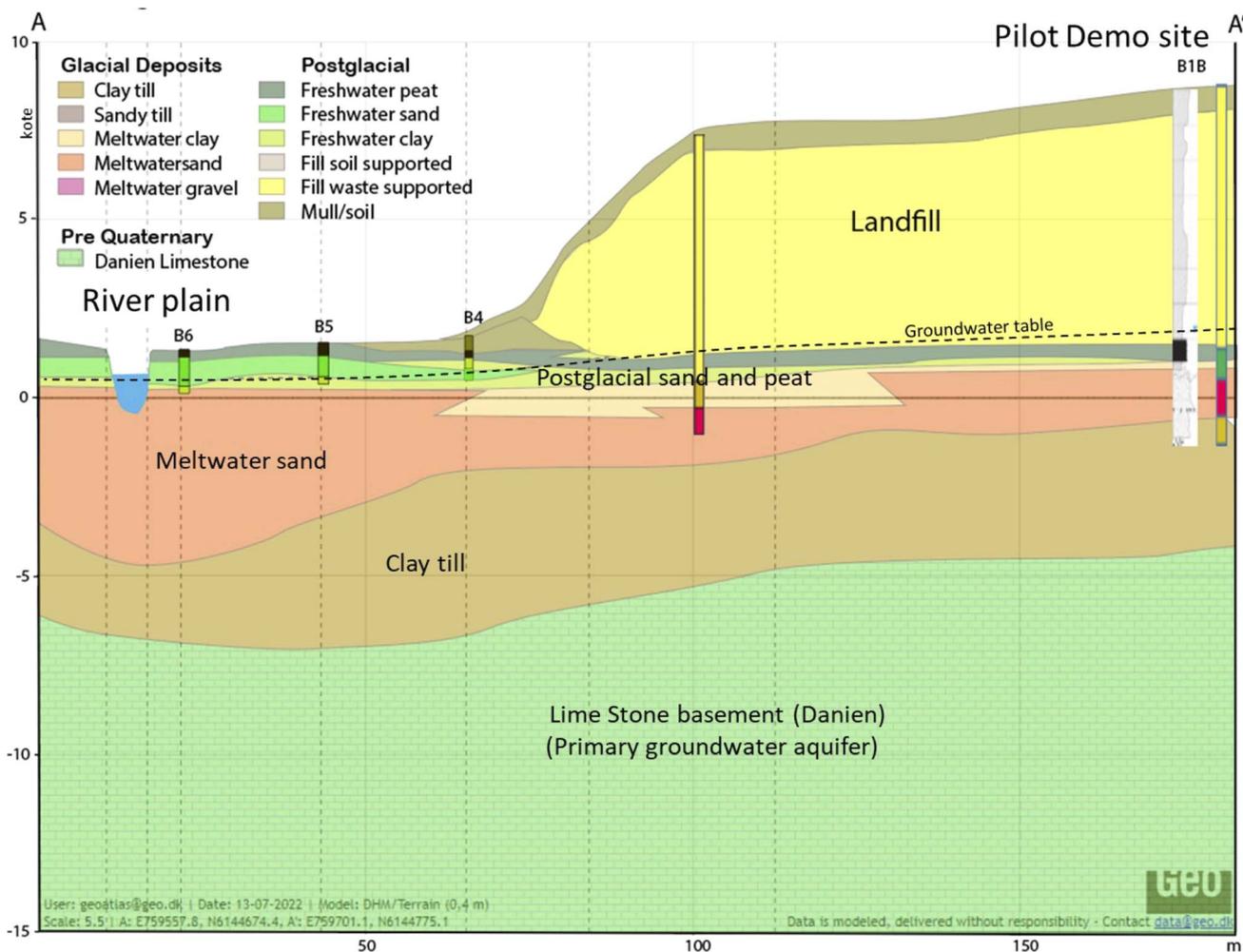
Fig. 3 Cross-section and geological settings from the Albech River to the landfill site.

Experimental setup of Winogradsky columns, characterization of microbial communities, and isolation of bacteria

Winogradsky columns[78] were used as microcosms to challenge microbial communities from the PFAS-contaminated Trelleborg site B1 (Fig. 1–3 and Table 1) in an attempt to isolate PFAS-resistant microorganisms and study the underlying mechanisms of resistance. Two sets of Winogradsky columns (without or with 2 mg per mL PFOA) were set up using soil sampled at 7.5 m of depth, and the columns were structured in an aqueous phase, a "top layer" and a "bottom layer" as described in Materials and methods. The columns were incubated for 2 months at room temperature. Then the "top layer" and the aqueous phase of the columns were analyzed by culture-based and culture-independent approaches in this study. Serial dilutions of the aqueous phase of the columns and native control soil were plated onto LB agar plates containing 2 mg per mL PFOA and in control LB agar plates without PFOA to determine microbial counts (Fig. 4). Bacteria resistant to PFOA were found in both the aqueous phase and the "top layer" of the PFOA-containing Winogradsky columns. In contrast, no bacteria

resistant to PFOA were isolated from the "bottom layer" of the columns. In particular, in the aqueous phase of the PFOA-containing Winogradsky columns, nearly identical microbial counts (approximately 7×10^6 CFU mL^{-1}) were detected on PFOA-containing and PFOA-free LB agar plates (Fig. 4A and B, green). In the aqueous phase of the PFOA-free Winogradsky columns, slightly lower microbial counts (approximately 2.5×10^6 CFU mL^{-1}) were observed on PFOA-free LB agar plates, whereas no colonies were observed on PFOA-containing LB agar plates (Fig. 4A and B, violet). In native soil, microbial counts of 3×10^5 CFU mL^{-1} were recorded on PFOA-free LB agar plates and no colonies on PFOA-containing LB agar plates (Fig. 4A and B, grey).

PFOA-containing LB agar plates were then used to isolate PFOA-resistant microorganisms. Colonies exhibited two distinct morphotypes, designated Tre-B and Tre-T, and a visual analysis of each morphotype showed a clear prevalence of Tre-T (approximately 7×10^6 CFU mL^{-1}) over Tre-B (approximately 2×10^5 CFU mL^{-1}) (Fig. 4C). Five colonies for each morphotype were then analyzed by rep-PCR (Fig. 4D). The results demonstrated identical profiles within each morphotype and different

Table 1 Results of chemical analyses, detailing the concentrations of PFAS observed at the 7.5 m sampling height of borehole B1

Parameters	Unit	B1–7.5 m
Dry weight	%	78.2
PFBA (perfluorbutanoicacid)	µg per kg dw	0.23
PFBS (perfluorbutansulfonicacid)	µg per kg dw	0.41
PFPeA (perfluorpentanoicacid)	µg per kg dw	1.1
PFPeS (perfluorpentansulfonicacid)	µg per kg dw	0.38
PFHxA (perfluorhexanoic acid)	µg per kg dw	0.96
PFHxS (perfluorhexansulfonoic acid)	µg per kg dw	4.9
PFHpA (perfluorheptanoic acid)	µg per kg dw	0.29
PFHpS (perfluorheptansulfonoic acid)	µg per kg dw	0.55
PFOA (perfluoroctanoic acid)	µg per kg dw	0.68
PFOS (perfluoroctansulfonoic acid)	µg per kg dw	45
6 : 2 FTS (fluortelomersulfonat)	µg per kg dw	1.5
PFOSA (perfluoroctansulfonamid)	µg per kg dw	0.33
PFNA (perfluornonanoic acid)	µg per kg dw	<0.10
PFNS (perfluornonansulfonoic acid)	µg per kg dw	<0.20
PFDA (perfluordekanoic acid)	µg per kg dw	0.31
PFDS (perflordekanesulfonoic acid)	µg per kg dw	0.18
PFUnDA (perfluorundecanoic acid)	µg per kg dw	0.15
PFUnDS (perfluorundecansulfonoic acid)	µg per kg dw	<1.0
PFDoDA (perfluordodecanoic acid)	µg per kg dw	0.24
PFDoDS (perfluordodekansulfonoic acid)	µg per kg dw	<1.0
PFTrDA (perfluortridekanoic acid)	µg per kg dw	<0.10
PFTrDS (perfluortridekansulfonoic acid)	µg per kg dw	<1.0
Sum af PFAS 4 excl. LOQ	µg per kg dw	51
Sum af PFAS excl. LOQ	µg per kg dw	57

profiles between the two morphotypes suggesting the presence of two distinct taxa. Therefore, two bacterial isolates, one for each morphotype, were subjected to whole-genome sequencing. MIC experiments showed that the Tre-B isolate was slightly more resistant than the Tre-T isolate to PFOA and the reference *E. coli* strain FB8. MIC values were 8 mg mL^{-1} for the Tre-B isolate, 7 mg mL^{-1} for the Tre-T isolate, and 6 mg mL^{-1} for *E. coli* FB8 (Fig. S2†). In contrast, the MIC measured using fluoride (NaF) was the same for *K. grimontii* Tre-B, *C. braakii* Tre-T, and *E. coli* FB8. However, the isolates *K. grimontii* Tre-B and *C. braakii* showed an MBC value of 1 M. This value for *E. coli* FB8 was half (0.5 M) (Fig. S2†).

To characterize the structure of the microbial communities in the PFOA-containing and PFOA-free Winogradsky columns, total DNA was extracted from the aqueous phase and the "top layer" of the columns and subject to 16S rRNA metabarcoding analysis (Fig. 5). The bacterial communities were analyzed at three different taxonomic levels: phyla, orders, and families.

In the PFOA-free columns, the most representative phyla (abundance >0.5%) at phylum level (Fig. 5A) were Firmicutes, Proteobacteria, Bacteroidetes, Chloroflexi, Spirochaetes, Actinobacteria, Synergistetes, Cloacimonetes, Armatimonadetes, Euryarchaeota, Tenericutes, and Deinococcus/unclassified Thermus. In the PFOA-containing columns, the most representative phyla were Proteobacteria, Firmicutes, Actinobacteria, Bacteroidetes, Chloroflexi, Cyanobacteria/Chloroplast, Acidobacteria, Euryarchaeota, and Synergistetes. Interestingly, Proteobacteria were much more abundant in the PFOA-containing columns than in the PFOA-free columns (81.11% *vs.* 22.56%).

Actinobacteria, Cyanobacteria/Chloroplast, Acidobacteria, Planctomycetes, Chlamydiae, Candidatus_Saccharibacteria, Parcubacteria, and Atribacteria were also more abundant in the PFOA-containing columns than in PFOA-free columns. In contrast, Firmicutes and Bacteroidetes were more abundant in PFOA-free columns than in PFOA-containing columns (42.22% *vs.* 9.70%; 16.52% *vs.* 1.41%). Chloroflexi, Synergistetes, Spirochaetes, and Cloacimonetes were also more abundant in the PFOA-free columns than in PFOA-containing columns.

At order level (Fig. 5B), the majority of Proteobacteria in the PFOA-containing columns were Enterobacteriales (79%), while this order was much less represented in the PFOA-free columns (0.037%). Rhizobiales, within the Proteobacteria phylum, were also more abundant in the PFOA-containing columns. Conversely, Caulobacterales, also belonging to the Proteobacteria phylum, was more abundant in the PFOA-free columns. Among Firmicutes, the orders Clostridiales, Bacillales, and Selenomonadales were much more represented abundant in the PFOA-free columns than in the PFOA-containing columns. In contrast, the order Lactobacillales was more abundant in the PFOA-containing columns (2%) than in the PFOA-free columns (0.43%). Other orders that were more abundant in the PFOA-free columns compared to the PFOA-containing columns were Bacteroidales, Anaerolineales, Desulfovibrionales, Desulfobacterales, Flavobacteriales, and Erysipelotrichales.

At family level (Fig. 5C), the most abundant family in the PFOA-containing columns was Enterobacteriaceae (79%). The relative abundance of this family was very low in the PFOA-free columns (0.037%). Carnobacteriaceae also were more represented in the PFOA-containing columns (1.87%) then in the PFOA-free columns (0.34%). In contrast, the relative abundance of Lachnospiraceae (phylum Firmicutes) was similar (about 2%) in both columns. Conversely, other families were more represented in the PFOA-free columns (>2%) than in PFOA-containing columns, including Caulobacteraceae, Porphyromonadaceae, Anaerolineaceae, Clostridiales_Incertae_Sedis_XI, Desulfovibrionaceae, Ruminococcaceae, Planococcaceae, Gracilibacteraceae, Desulfobulbaceae, Bacillaceae, Spirochaetaceae, Acidaminococcaceae and Peptococcaceae.

The high relative abundance of Enterobacteriaceae in the PFOA-containing columns was consistent with the culture-based analysis that led to the isolation of two strains (Tre-B and Tre-T) of this family.

Whole genome sequence and characterization of *Klebsiella grimontii* strain Tre-B

A total of 7 348 974 reads were sequenced and the genome assembly of strain Tre-B was represented by 36 contigs with a N_{50} value of 456 983 bp and a N_{75} value of 248 966 bp; the largest contig was 841 358 bp. The average coverage was >90-fold. The combined length was 5 886 764 bp with a G + C content of 55.9% (Table 2). Based on Genome Taxonomy Database, genome sequence of strain Tre-B showed the highest identity (99.26%) with the that of *Klebsiella grimontii* reference strain 06D021 (accession GCA900200035.1). Rapid genome
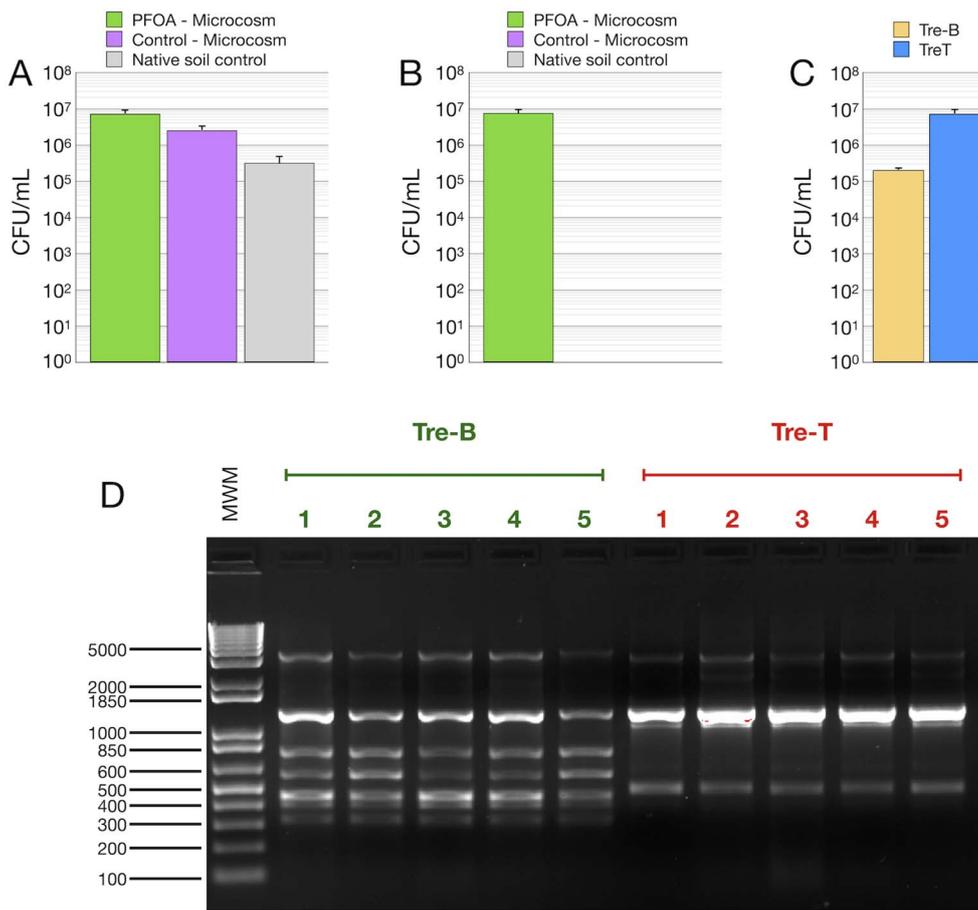
© 2025 The Author(s). Published by the Royal Society of Chemistry

Environ. Sci.: Adv., 2025, **4**, 1444–1476 | **1453**

Fig. 4 CFU quantification and molecular characterization of the isolates. (A and B) The bacterial load in the microcosms was analyzed using the serial dilution method and LB agar medium (A) or LB agar medium supplemented with PFOA (2 mg mL^{-1}) (B). (C) The two bacterial morphotypes isolated using PFOA-enriched LB agar were counted separately to estimate the abundance of Tre-B morphotype *versus* Tre-T morphotype. (D) 5 colonies of each morphotype were analyzed by rep-PCR which demonstrated that the colonies were groupable in two genomic fingerprints. MWM = molecular weight marker.

annotation was performed with Prokka.[62] Annotation features identified with Prokka v1.14.6 (ref. 62) includes 5354 DNA coding sequences (CDSs), 20 rRNAs, 81 tRNAs (Table 2). Annotation features identified with DFAST v5.0.2 (ref. 63) identified a total of 5384 CDSs, 9 rRNAs, 81 tRNAs and one CRISPR locus (Table 2). According to these results, the annotation was manually implemented, and results are reported in Table S1.†

K. grimontii is a newly identified species closely related to *Klebsiella oxytoca*.[79] *K. oxytoca* has a chromosomally encoded β-lactamase gene (*bla*$_{OXY}$) that confers resistance to amino- and carboxypenicillins.[80] This gene diversified in parallel to housekeeping genes in species closely related to *K. oxytoca*, and variants *bla*$_{OXY-1}$ to *bla*$_{OXY-7}$ allowed to classify these closely related bacteria into seven phylogenetic lineages named from Ko1 to Ko7. *K. oxytoca* corresponds to phylogroup Ko2, while *K. grimontii* corresponds to phylogroup Ko6.[79] Resistance Gene Identifier[64] predicted the presence of *bla*$_{OXY-6-1}$ gene in strain Tre-B (Table 3) confirming the correct assignment to the species *K. grimontii*. Consistent with this result, MIC experiments showed that growth of *K. grimontii* Tre-B was not inhibited by 500 mg per mL ampicillin (Fig. S2†). Resistance Gene Identifier

also predicted acquired resistance to very wide range of antibiotics, disinfecting agents and antiseptics (Tables 3 and S2†). In particular, a plethora of genes are involved in resistance to fluoroquinolones, coding for different antibiotic efflux pumps belonging to the major facilitator superfamily (MFS) (KpnGH-TolC) or to the resistance-nodulation-cell division (RND) superfamily (AdeFGH, OqxA, AcrAB-TolC) and to MFS and RND antibiotic efflux pump regulators (Tables 3 and S2†). It may be also noted the presence of a gene (OKNGJBID03127) encoding methyl viologen (*i.e.*, the herbicide Paraquat) resistance protein SmvA, an MFS transporter.

Whole genome sequence of *K. grimontii* Tre-B showed that it has the potential to be a human pathogen. Analysis by antiSMASH 7.0 (ref. 68) revealed that it contains the entire biosynthetic gene cluster for the potent cytotoxin kleboxymycin (Fig. 6 and Table 4), while genes for other virulence factors were identified by VirulenceFinder-2.0 Server[67] and PathogenFinder.[65,66] VirulenceFinder-2.0 Server identified the gene encoding the lipoprotein NlpI precursor as virulence factor according to previous data showing an involvement of lipoprotein NlpI in the virulence of adherent invasive *Escherichia*
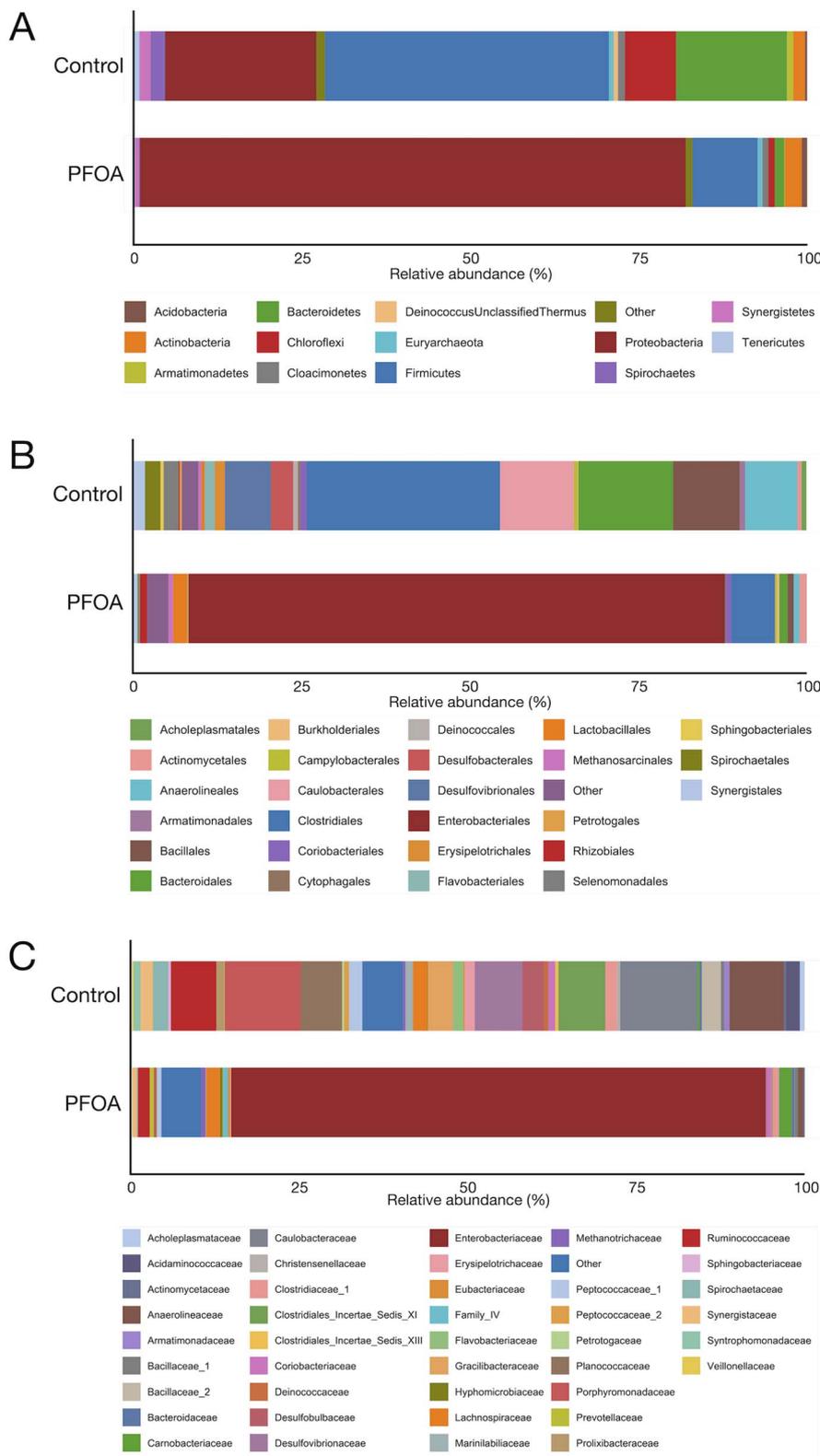
Fig. 5 Composition of microbial communities in the PFOA-containing and PFOA-free Winogradsky columns: phyla level (A), order level (B), family level (C).

coli strain isolated from a patient with Crohn's disease.[81] PathogenFinder identified a long list of putative virulence factors and provided a probability score of being a human pathogen of 0.858 (as a reference, the probability score of *Salmonella enterica* sv. Typhimurium LT2 is 0.937). Among the virulence factors identified by PathogenFinder, adhesins,

© 2025 The Author(s). Published by the Royal Society of Chemistry

Environ. Sci.: Adv., 2025, **4**, 1444–1476 | **1455**

Table 2 Features of *Klebsiella grimontii* strain Tre-B and *Citrobacter braakii* strain Tre-T genome sequences, and features of pKGTreB plasmid revealed by MobileElementFinder. Number of CDSs, rRNAs, and tRNAs show the two values resulted from Prokka/DFAST annotations

Feature	Value (Tre-B)	Value (Tre-T)	Value (pKGTreB)
Total sequence length (bp)	5 887 560	4 936 210	87 115
Number of contigs	36	28	6
Largest contig (bp)	841 358	1 837 299	50 714
N_{50} (bp)	456 983	484 747	50 714
Gap ratio (%)	0.452242	0.000000	0.000000
GC content (%)	55.9	52.2	51.9
Number of CDSs	5354/5384	4581/4563	88
Average protein length	320.0	319.5	260.80
Coding ratio (%)	87.8	88.6	79.0
Number of rRNAs	20/9	9/9	0
Number of tRNAs	81/81	75/75	0
Number of CRISPRs	1	1	0
IncR (position: nt, reverse/forward)			44 742–44 992
ISEcl1 (position: nt, reverse/forward)			38 327–39 662 forward
ISKpn34 (position: nt, reverse/forward)			14 837–16 025 reverse
IS903 (position: nt, reverse/forward)			1139–2195 forward
IS903 (position: nt, reverse/forward)			753–1805 forward
IS26 (position: nt, reverse/forward)			2–821 forward

fimbrial systems, flagellin, invasins, cell invasion proteins, secretion system structural proteins and effectors, LPS modification enzymes, hemolysins, iron uptake systems, phospholipases, and proteins involved in host sialic acid metabolism and uptake were found.

Genes coding for structural components of metabolosomes were also found. Metabolosomes are bacterial microcompartments (BMCs) forming polyhedral bodies, which consist of a single-layer proteinaceous shell that encapsulates both enzymes and metabolites facilitating specific catabolic pathways in a protected micro-environment.[82] In general, these pathways are characterized by the presence of oxygen sensitive metal co-factor containing enzymes, such as coenzyme B_{12}-dependent and glycyl-radical enzymes, and BMCs may facilitate these pathways by an O_2 exclusion mechanism.[83,84] The most well studied metabolosomes are the 1,2-propanediol utilization (*pdu*), the ethanolamine utilization (*eut*), the choline utilization (*cut*), and the glycyl radical propanediol (*grp*) catabolic BMCs, which are found in several strains of *Salmonella enterica* and *Escherichia coli*[82] (Fig. 7, S3 and Table S3†).

K. grimontii Tre-B contains three BMC loci (Table S1†): *pdu* BMC locus, *eut* BMC locus and choline utilization (*cut*) BMC locus (Fig. 7 and Table S3†) characterized in *E. coli* 536 and *Proteus mirabilis*.[85,86] *cut* BMC loci were identified in 21 of 25 fully sequenced *K. grimontii* genomes, suggesting a broad distribution among strains of this species (Table S4†). *cut* enzymes choline trimethylamine lyase (CutC) and its activating enzyme (CutD) were also found in *K. pneumoniae*,[87] and structural shell BMC proteins have been recently characterized in this microorganism.[88] *cut* BMCs have been implicated in diseases in humans, because they catabolize choline to trimethylamine (TMA) plus ethanol or acetate, and they are a major source of TMA in the intestine. TMA is further metabolized in the liver to trimethylamine-*N*-oxide (TMAO), whose high levels have been associated with various diseases, including non-alcoholic fatty liver disease,[89] cardiovascular disease and atherosclerosis,[90,91] kidney disease,[92] and diabetes.[93]

On the other hand, the presence of *dmsA* coding for dimethyl sulfoxide/trimethylamine *N*-oxide reductase in the genome of *K. grimontii* Tre-B (Fig. 8 and Table S1†) may allow this microorganism to use TMAO as an alternative electron acceptor in anaerobic respiration,[94] and in the genome of *K. grimontii* Tre-B it may be noted the presence of *dmsA* coding for dimethyl sulfoxide/trimethylamine *N*-oxide reductase, a molybdopterin-dependent oxidoreductase. *dmsA* maps in a genomic region encompassing genes involved in biosynthesis of lipoic acid from octanoic acid (*lipA*, *lipB*, *pagP*), fluoride ion transport (*crcB*), general stress (*uspG*), cold stress (*cspE*), oxidative stress (*ahpF*, *ahpC*), glutathione metabolism (*ybeM*) and methionine metabolism and savage pathway (*ybdO*, *ybdM*, *ybdL*, *mntC*, *mntD*) (Fig. 8). In particular, the fluoride ion transport may be relevant for resistance to PFOA in presence of activities that defluorinate this compound.

MobileElementFinder[69] detected the presence of IncR-group plasmid and numerous mobile genetic elements in the genome of *K. grimontii* Tre-B. The IncR-group plasmid (named pKGTreB) has a total length of 87 115 bp and contains 88 predicted CDSs, including numerous insertion sequences (ISEcl1, ISKpn34, IS903, IS26) (Table 2), and, notably, many genes involved in resistance to arsenic, copper, mercury and silver (Table 5), and a gene coding for a putative glycosyl transferase (*epsJ*) that in *Bacillus subtilis* 168 has been involved in biofilm matrix formation.[95] pKGTreB also contains genes coding for proteins involved in maltose/maltodexrin transport and metabolism, and type II toxin-antitoxin system (*vapB*/*vapC*). Resistance against silver was confirmed in laboratory experiments. In particular, while the MIC of silver nitrate was the same in *K. grimontii* Tre-B and reference *E. coli* FB8 (0.63 mM), and lower in *Citrobacter braakii* Tre-T (0.08 mM), the MBC of this compound was much higher in *K. grimontii* Tre-B (320 mM) as compared to

Table 3   Acquired resistance to antimicrobial compounds in *K. grimontii* Tre-B and *C. braakii* Tre-T predicted by Resistance Gene Identifier

BestHitARO	Drug class	Tre-B	Tre-T
adeF	Fluoroquinolone antibiotic; tetracycline antibiotic	+	−
ArnT	Peptide antibiotic	+	−
eptB	Peptide antibiotic	+	−
fosA5	Fluoroquinolone antibiotic; aminoglycoside antibiotic; phosphonic acid antibiotic	+	−
Klebsiella pneumoniae KpnG	Macrolide antibiotic; fluoroquinolone antibiotic; aminoglycoside antibiotic; carbapenem; cephalosporin; penam; peptide antibiotic; penem	+	−
Klebsiella pneumoniae KpnH	Macrolide antibiotic; fluoroquinolone antibiotic; aminoglycoside antibiotic; carbapenem; cephalosporin; penam; peptide antibiotic; penem	+	−
LptD	Peptide antibiotic; aminocoumarin antibiotic; rifamycin antibiotic	+	−
Morganella morganii gyrB conferring resistance to fluoroquinolones	Fluoroquinolone antibiotic	+	−
oqxA	Fluoroquinolone antibiotic; glycylcycline; tetracycline antibiotic; diaminopyrimidine antibiotic; nitrofuran antibiotic	+	−
OXY-6-1	Monobactam; cephalosporin; penam	+	−
qacJ	Disinfecting agents and antiseptics	+	−
baeR	Aminoglycoside antibiotic; aminocoumarin antibiotic	+	+
CRP	Macrolide antibiotic; fluoroquinolone antibiotic; penam	+	+
emrR	Fluoroquinolone antibiotic	+	+
Escherichia coli AcrAB-TolC with MarR mutations conferring resistance to ciprofloxacin and tetracycline	Fluoroquinolone antibiotic; cephalosporin; glycylcycline; penam; tetracycline antibiotic; rifamycin antibiotic; phenicol antibiotic; disinfecting agents and antiseptics	+	+
Escherichia coli EF-Tu mutants conferring resistance to pulvomycin	Elfamycin antibiotic	+	+
Escherichia coli UhpT with mutation conferring resistance to fosfomycin	Phosphonic acid antibiotic	+	+
H-NS	Macrolide antibiotic; fluoroquinolone antibiotic; cephalosporin; cephamycin; penam; tetracycline antibiotic	+	+
Haemophilus influenzae PBP3 conferring resistance to beta-lactam antibiotics	Cephalosporin; cephamycin; penam	+	+
Klebsiella pneumoniae KpnE	Macrolide antibiotic; aminoglycoside antibiotic; cephalosporin; tetracycline antibiotic; peptide antibiotic; rifamycin antibiotic; disinfecting agents and antiseptics	+	+
Klebsiella pneumoniae KpnF	Macrolide antibiotic; aminoglycoside antibiotic; cephalosporin; tetracycline antibiotic; peptide antibiotic; rifamycin antibiotic; disinfecting agents and antiseptics	+	+
leuO		+	+

Table 3 (*Contd.*)

BestHitARO	Drug class	Tre-B	Tre-T
	nucleoside antibiotic; disinfecting agents and antiseptics		
marA	Fluoroquinolone antibiotic; monobactam; carbapenem; cephalosporin; glycylcycline; cephamycin; penam; tetracycline antibiotic; rifamycin antibiotic; phenicol antibiotic; penem; disinfecting agents and antiseptics	+	+
msbA	nitroimidazole antibiotic	+	+
rsmA	Fluoroquinolone antibiotic; diaminopyrimidine antibiotic; phenicol antibiotic	+	+
vanG	Glycopeptide antibiotic	+	+
CMY-70	Cephamycin	−	+
emrB	Fluoroquinolone antibiotic	−	+
Escherichia coli acrA	Fluoroquinolone antibiotic; cephalosporin; glycylcycline; penam; tetracycline antibiotic; rifamycin antibiotic; phenicol antibiotic; disinfecting agents and antiseptics	−	+
Escherichia coli EF-Tu mutants conferring resistance to pulvomycin	Elfamycin antibiotic	−	+
Escherichia coli GlpT with mutation conferring resistance to fosfomycin	Phosphonic acid antibiotic	−	+
Escherichia coli mdfA	Tetracycline antibiotic; disinfecting agents and antiseptics	−	+
kdpE	Aminoglycoside antibiotic	−	+
mdtB	Aminocoumarin antibiotic	−	+
mdtG	Phosphonic acid antibiotic	−	+
PmrF	Peptide antibiotic	−	+

E. coli FB8 (0.15 mM), and lower in *C. braakii* Tre-T (5 mM) (Fig. S2†). In contrast, the MIC values of chromium, aluminum, nickel, and copper were the same in *K. grimontii* Tre-B and *C. braakii* Tre-T.

The genome sequence of *K. grimontii* Tre-B also showed that it has a considerable potential for degradation of a wide array of aromatic compounds and recalcitrant chemicals (Table 6). A total of 14 monooxygenase- and 18 dioxygenase-encoding genes
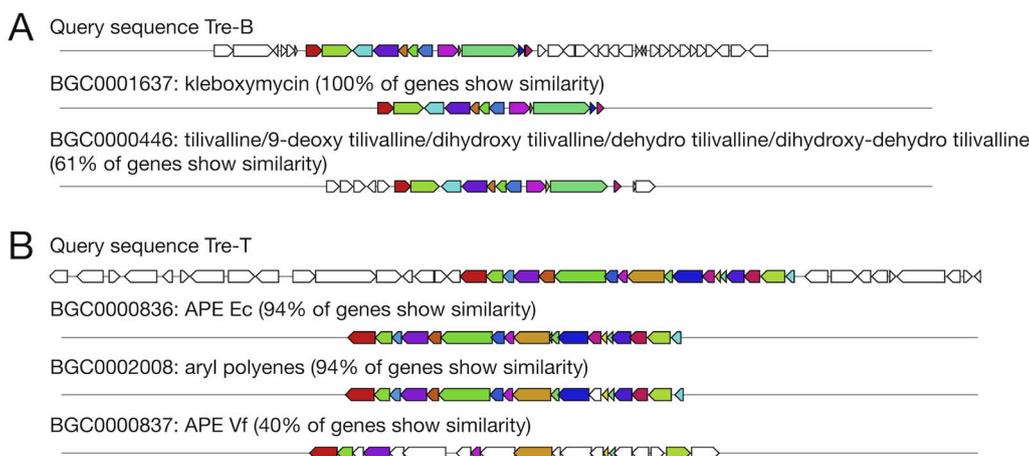

Fig. 6 Kleboxymycin gene cluster revealed by antiSMASH in the genome of *K. grimontii* Tre-B (A) and aryl polyene gene cluster revealed by antiSMASH in the genome of *C. braakii* Tre-T (B).

© 2025 The Author(s). Published by the Royal Society of Chemistry

Table 4 Secondary metabolites in *K. grimontii* Tre-B and *C. braakii* Tre-T predicted by antiSMASH

Region	Type	From	To	Most similar known cluster	Similarity	Strain
Region 12.1	Thiopeptide	245 295	271 573	O-Antigen saccharide	14%	Tre-B
Region 24.1	RiPP	27 708	36 416			Tre-B
Region 28.1	NRPS	70 758	113 466	Kleboxymycin NRP	100%	Tre-B
Region 28.2	T1PKS, NRP-metallophore, NRPS	176 031	239 201	Yersiniabactin NPR + polyketide	16%	Tre-B
Region 29.1	NRP-metallophore	148 067	202 054	Enterobactin NPR	100%	Tre-B
Region 4.1	Aryl polyene	280 804	324 400	APE Ec	94%	Tre-T
Region 12.1	NRP-metallophore, NRPS	275 693	329 439	Enterobactin NRP	100%	Tre-T
Region 16.1	Thiopeptide	1 792 500	1 818 790	O-Antigen saccharide	14%	Tre-T

were annotated in the genome sequence, which are involved in different pathways, including: (i) degradation of exogenous pyrimidines as the sole nitrogen source; (ii) degradation of homo-protocatechuate; (iii) degradation of 4-hydroxyphenylacetate; (iv) degradation of benzoate and 2-halo (F, Br, Cl, I)-benzoate to catechol; (v) degradation of catechol to beta-ketoadipate; (vi) degradation of beta-ketoadipate to succinyl-CoA and acetyl-CoA; (vii) degradation of 4-hydroxybenzoate to protocatechuate; (viii) degradation of 3-hydroxybenzoate *via* gentisate to pyruvate and fumarate; (ix) degradation of nitrilo-triacetate (NTA) to iminodiacetate and glyoxylate; (x) degradation of aliphatic sulfonates to utilize dimethyl sulfide and methanesulfonate as a carbon and energy and/or sulfur source; (xi) degradation of taurine as an alternative sulfur source for growth in the absence of sulfate; (xii) degradation and metabolism of quercetin and other plant flavonoids. It may be also noted the presence of duplicated genes coding for validamycin

A dioxygenase that is responsible for transformation of the antibiotic validamycin A to validamycin B, which is less active (Table 6).

Whole genome sequence and characterization of *Citrobacter braakii* strain Tre-T

A total of 8 193 946 reads were sequenced for strain Tre-T and the genome assembly was represented by 28 contigs with a N_{50} value of 484 747 bp and a N_{75} value of 413 051 bp; the largest contig was 1 837 299 bp. The average coverage was >90-fold. The combined length was 4 936 210 bp with a G + C content of 52.2% (Table 2). Based on Genome Taxonomy Database, genome sequence of strain Tre-T showed the highest identity (98.71%) with the that of *Citrobacter braakii* strain ATCC 51113 (accession GCA002075345.1). Rapid genome annotation was performed with Prokka.[62] Annotation features identified with Prokka v1.14.6 (ref. 62) includes a 4581 DNA coding sequences (CDSs),
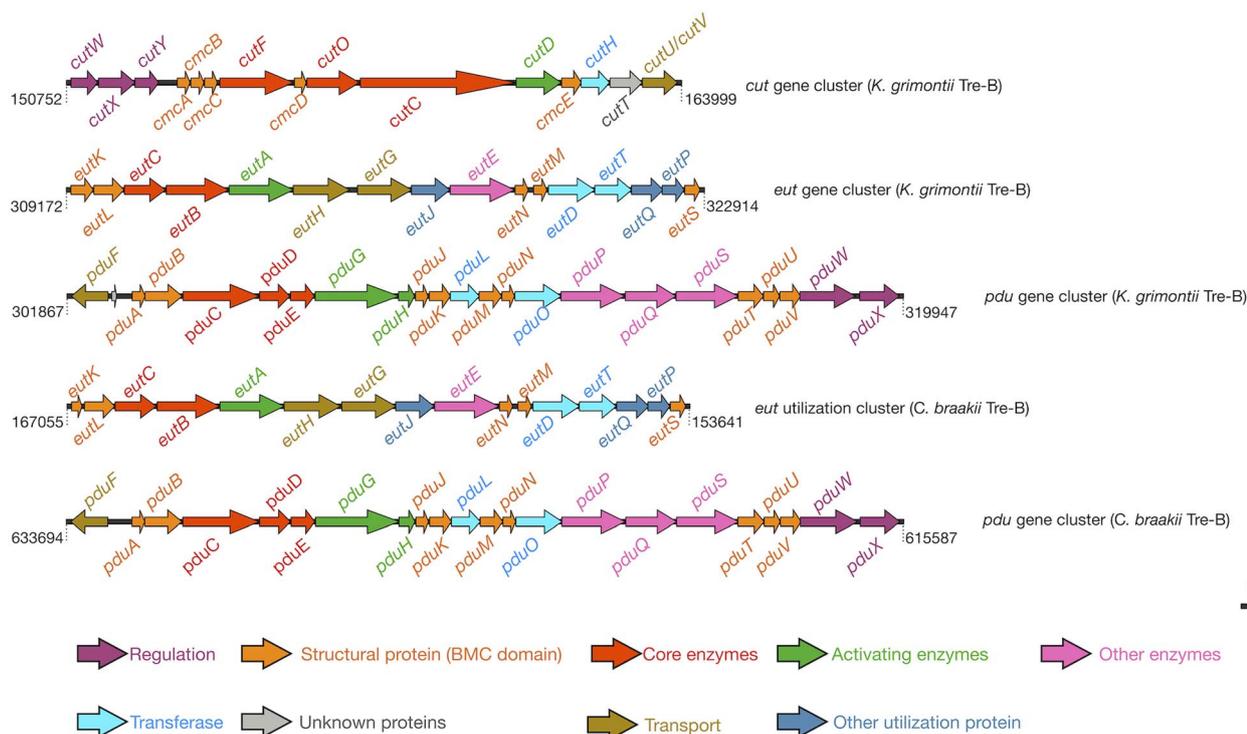
Fig. 7 Genetic maps of *cut, pdu* and *eut* loci of *K. grimontii* Tre-B, and *pdu* and *eut* loci of *C. braakii* Tre-T.

© 2025 The Author(s). Published by the Royal Society of Chemistry
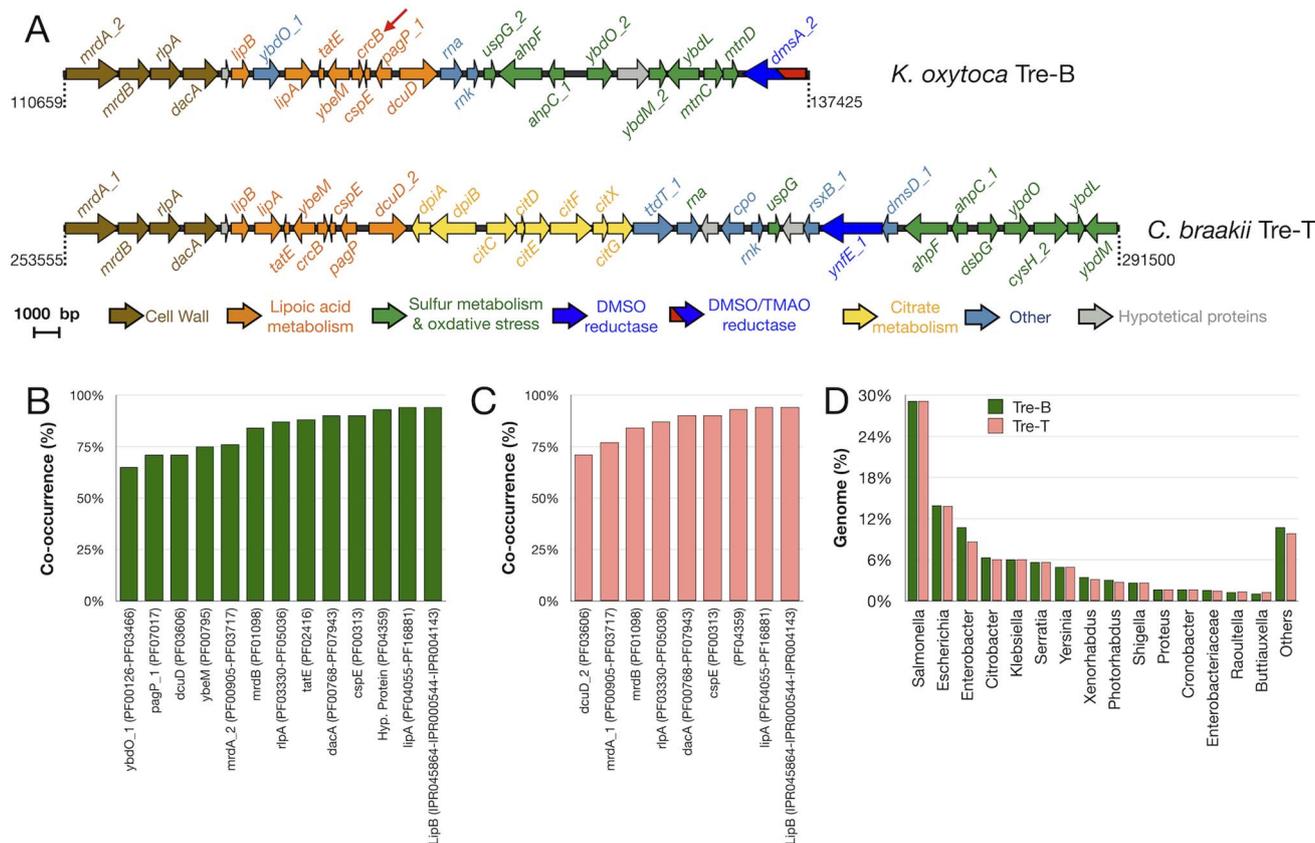
Environ. Sci.: Adv., 2025, **4**, 1444–1476 | **1459**

Fig. 8 Genetic mapping and conservation of protein-coding regions involved in lipoic acid metabolism and fluoride transport. (A) Genetic maps of *K. grimontii* Tre-B and *C. braakii* Tre-T. The red arrow highlights the CrcB protein (F⁻ specific ion channel). (B and C) Co-occurrence of conserved genes. The data set was generated by inputting the CrcB protein sequence of *K. grimontii* Tre-B (OKNGJBID_03358) and *C. braakii* Tre-T (LBFIJIGF_01727) and using the EFI-EST and EFI-GNT tools. (D) Most abundant bacterial genera in the data set obtained from EFI-EST/EFI-GNT.

13 rRNAs, 75 tRNAs (Table 2). Annotation features identified with DFAST v5.0.2 (ref. 63) identified a total of 4563 CDSs, 9 rRNAs, 75 tRNAs and one CRISPR locus (Table 2). According to these results, annotation was then manually implemented, and results are reported is reported in Table S5.†

C. braakii is a species belonging to the large *Citrobacter freundii* complex.[96] As with *K. grimontii*, concern is growing about the environmental spread of these bacteria as they are acquiring multidrug resistance.[97,98] Indeed, the analysis of the genome of *C. braakii* Tre-T with Resistance Gene Identifier allowed to predict acquired resistance to very wide range of antibiotics, disinfecting agents and antiseptics (Tables 3 and S6†). In particular, factors associated with resistance to fluoroquinolones include the presence of the acridine-resistance proteins A and B (AcrAB) and the multidrug efflux pump outer membrane factor TolC (AcrAB-TolC) with MarR mutations conferring resistance to ciprofloxacin and tetracycline, also present in *K. grimontii* Tre-B. It may be seen that in several members of the γ-Proteobacteria this efflux pump confers resistance to a wide range of toxic compounds such as antibiotics, surfactants, dyes, detergents, and disinfectants which are not found in the natural environment of these bacteria.[99–101]

The analysis of the genome of *C. braakii* Tre-T also revealed that the genomic region encompassing genes involved in biosynthesis of lipoic acid from octanoic acid (*lipA*, *lipB*, *pagP*), fluoride ion transport (*crcB*), general stress (*uspG*), cold stress (*cspE*), oxidative stress (*ahpF*, *ahpC*), glutathione metabolism (*ybeM*) and methionine metabolism (*ybdO*, *ybdM*, *ybdL*) have a similar arrangement with respect to the syntenic region of *K. grimontii* Tre-B. However, the *K. grimontii* Tre-B gene *dmsA* coding for dimethyl sulfoxide/trimethylamine *N*-oxide reductase was notably replaced by a different molybdopterin-dependent oxidoreductase that is not able to use TMAO (Fig. 8). The analysis of the genome of *C. braakii* Tre-T revealed two BMC loci (Table S5†): the *pdu* BMC locus and the *eut* BMC locus. At variance with *K. grimontii* Tre-B, the *cut* BMC locus was absent (Fig. 7 and Table S3†). *C. braakii* Tre-T as well as *K grimontii* Tre-B also present loci *eut* and *pdu* (Fig. 7). These loci are extremely similar to those of *K grimontii* Tre-B and the encoded proteins are homologous to those identified in *S. enterica* LT2.

Whole genome sequence of *C. braakii* Tre-T showed that it has the potential to be a human pathogen. antiSMASH 7.0 (ref. 68) revealed that it contains an aryl polyene biosynthetic gene cluster (Fig. 6 and Table 4), 94% similar to that found in *E. coli* CFT073. Aryl polyene are specialized polyunsaturated carboxylic

Table 5 Relevant CDSs of pKGTreB plasmid

Locustag (genome)	Locustag (plasmid)	CDS (bp)	Gene	Product
OKNGJBID02184	MGA88/89	924		IS5 family transposase IS903
OKNGJBID02185	MGA58	2967		Tn3-like element ISPa38 family transposase
OKNGJBID02186	MGA59	291		Nucleotidyltransferase
OKNGJBID02187	MGA60	402		DUF86 domain-containing protein
OKNGJBID02188	MGA61	357		Cupin domain-containing protein
OKNGJBID02189	MGA62	327		Hypothetical protein
OKNGJBID02190	MGA63	501		Hypothetical protein
OKNGJBID02191	MGA64	372		Hypothetical protein
OKNGJBID02192	MGA65	558	*hin*	Recombinase family protein
OKNGJBID02193	MGA66	750	*epsJ*	Glycosyltransferase EpsJ
OKNGJBID02194	MGA67	828	*usp*	Universal stress protein
OKNGJBID02195	MGA68	1479		SulP family inorganic anion transporter
OKNGJBID02196	MGA69	249		Recombinase family protein
OKNGJBID02197	MGA70	2985		Tn3-like element TnAs3 family transposase
OKNGJBID02198		123		Hypothetical protein
OKNGJBID02199	MGA71	126		Hypothetical protein
OKNGJBID02200	MGA72	795		IS3 family transposase ISKpn34
OKNGJBID02201	MGA73	2796		Tn3-like element Tn3 family transposase
OKNGJBID02202	MGA74	573		Recombinase family protein
OKNGJBID02203	MGA75	405		Hypothetical protein
OKNGJBID02204	MGA76	426	*arsC*	Glutaredoxin-dependent arsenate reductase
OKNGJBID02205	MGA77	1290	*arsB*	Arsenite efflux transporter membrane subunit ArsB
OKNGJBID02206	MGA78	1752	*arsA*	Arsenite efflux transporter ATPase subunit ArsA
OKNGJBID02207	MGA79	363	*arsD*	Arsenite efflux transporter metallochaperone ArsD
OKNGJBID02208	MGA80	354	*arsR*	As(III)-sensing metalloregulatory transcriptional repressor ArsR
OKNGJBID02209	MGA82	501	*ftnA*	Non-heme ferritin-like protein
OKNGJBID02210	MGA90	705		IS6-like element IS26 family transposase
OKNGJBID02211		1890		Tn3 family transposase
OKNGJBID02212	MGA84	1326	*amyB*	Alpha-amylase family glycosyl hydrolase
OKNGJBID02213	MGA85	1188	*malE*	Maltose/maltodextrin ABC transporter substrate-binding protein MalE
OKNGJBID02214	MGA90	705		IS6-like element IS26 family transposase
OKNGJBID02215	MGA1	558	*hin*	Recombinase family protein
OKNGJBID02216	MGA2	213		DUF3330 domain-containing protein
OKNGJBID02217	MGA3	237	*merE*	Broad-spectrum mercury transporter MerE
OKNGJBID02218	MGA4	366	*merD*	Mercury resistance co-regulator MerD
OKNGJBID02219	MGA5	1686	*merA*	Mercury(II) reductase
OKNGJBID02220	MGA6	426	*merC*	Organomercurial transporter MerC
OKNGJBID02221	MGA7	276	*merP*	Mercury resistance system periplasmic binding protein MerP
OKNGJBID02222	MGA8	411	*merT*	Mercuric ion transporter MerT
OKNGJBID02223	MGA9	456	*merR*	Hg(II)-responsive transcriptional regulator
OKNGJBID02224	MGA10	1083		IS110 family transposase
OKNGJBID02225	MGA12	1524		Group II intron reverse transcriptase/maturase
OKNGJBID02226	MGA14	285		IS3 family transposase
OKNGJBID02227	MGA15	417	*vapC*	Type II toxin-antitoxin system VapC family toxin
OKNGJBID02228	MGA16	231	*vapB*	Type II toxin-antitoxin system VapB family antitoxin
OKNGJBID02229	MGA17	378		Transposase
OKNGJBID02230	MGA18	348		IS66 family insertion sequence element accessory protein TnpB
OKNGJBID04814	MGA19	690		IS66-like element ISEc8 family transposase
OKNGJBID04815	MGA20	180	*parD*	Type II toxin-antitoxin system ParD family antitoxin
OKNGJBID04816	MGA21	99		Hypothetical protein
OKNGJBID04817	MGA22	435	*pcoE*	Copper resistance system metallochaperone PcoE
OKNGJBID04818	MGA23	1401	*pcoS*	Copper resistance membrane spanning protein PcoS
OKNGJBID04819	MGA24	681	*pcoR*	Copper response regulator transcription factor PcoR
OKNGJBID04820	MGA25	930	*pcoD*	Copper resistance inner membrane protein PcoD
OKNGJBID04821	MGA26	381	*pcoC*	Copper resistance system metallochaperone PcoC
OKNGJBID04822	MGA27	897	*pcoB*	Copper resistance outer membrane transporter PcoB
OKNGJBID04823	MGA28	1818	*pcoA*	Multicopper oxidase PcoA
OKNGJBID04824	MGA29	450		Copper resistance protein
OKNGJBID04825	MGA30	738		Peptidoglycan DD-metalloendopeptidase family protein
OKNGJBID04826	MGA31	198		DUF2933 domain-containing protein
OKNGJBID04827	MGA32	2442	*silP*	Ag(+)-translocating P-type ATPase SilP
OKNGJBID04828	MGA33	441		DUF411 domain-containing protein
OKNGJBID04829	MGA34	3147	*silA*	Cu(+)/Ag(+) efflux RND transporter permease subunit SilA

© 2025 The Author(s). Published by the Royal Society of Chemistry

Environ. Sci.: Adv., 2025, **4**, 1444–1476 | **1461**

Table 5 (Contd.)

Locustag (genome)	Locustag (plasmid)	CDS (bp)	Gene	Product
OKNGJBID04830	MGA35	1293	silB	Cu(+)/Ag(+) efflux RND transporter periplasmic adaptor subunit SilB
OKNGJBID04831	MGA36	354	cusF	Cation efflux system protein CusF
OKNGJBID04832	MGA37	1386	silC	Cu(+)/Ag(+) efflux RND transporter outer membrane channel SilC
OKNGJBID04833	MGA38	681	silR	Copper/silver response regulator transcription factor SilR
OKNGJBID04834	MGA39	1476	silS	Copper/silver sensor histidine kinase SilS
OKNGJBID04835	MGA40	432	silE	Silver-binding protein SilE
OKNGJBID04836	MGA41	234		Hypothetical protein
OKNGJBID04837	MGA42	915		HNH endonuclease
OKNGJBID04838		255		Hypothetical protein
OKNGJBID04839	MGA43	396		Hypothetical protein
OKNGJBID04840	MGA44	882		Hypothetical protein
OKNGJBID04841	MGA45	564		Hypothetical protein
OKNGJBID04842	MGA46	582		Hypothetical protein
OKNGJBID04843	MGA47	351		Hypothetical protein
OKNGJBID04844	MGA48	744		Hypothetical protein
OKNGJBID04845	MGA49	777		Site-specific integrase
OKNGJBID04846	MGA50	258		Hypothetical protein
OKNGJBID04847	MGA51	867	repE	Replication initiation protein RepE
OKNGJBID04848	MGA52	270		Hypothetical protein
OKNGJBID04849	MGA53	1206	parA	AAA family ATPase
OKNGJBID04850	MGA54	975	parB	ParB family protein
OKNGJBID04851	MGA56	276		IS1-like element transposase
OKNGJBID04852	MGA57	267		IS1 family transposase
OKNGJBID04853	MGA57	267		IS1 family transposase
OKNGJBID04854	MGA56	276		IS1-like element transposase

acids that increase protection from oxidative stress and contribute to biofilm formation in pathogenic *E. coli* strains.[102] VirulenceFinder-2.0 Server[67] identified the gene encoding the lipoprotein NlpI precursor as virulence factor,[81] also found in also present in *K. grimontii* Tre-B.

PathogenFinder[65,66] identified a long list of putative virulence factors and provided a probability score of being a human pathogen of 0.868 (as a reference, the probability score of *Salmonella enterica* sv. Typhimurium LT2 is 0.937). Among the virulence factors identified by PathogenFinder, Vi polysaccharide biosynthesis protein TviE, also found in *S. enterica* subsp. enterica serovar Parathyphi C, and hemolysin HylD were found.

In addition to *nlpI*, MobileElementFinder[69] detected the presence of bla_{CMY-82} and $bla_{CMY-101}$ to many beta-lactams and their associations (ampicillin + clavulanic acid, ceftazidime, ticarcillin + clavulanic acid, ampicillin, piperacillin + tazobactam, cefoxitin, amoxicillin, ticarcillin, cefotaxime, piperacillin, amoxicillin + clavulanic acid), and *traT* encoding an outer membrane protein that is involved in resistance to complement.

The genome sequence of *C. braakii* Tre-T also showed that it has a potential for degradation of some aromatic compounds and recalcitrant chemicals (Table 7). A total of 7 monooxygenase- and 8 dioxygenase-encoding genes were annotated in the genome sequence, which are involved in different pathways, including: (i) degradation of 3-phenylpropanoate; (ii) degradation of 3-hydroxybenzoate *via* gentisate to pyruvate and fumarate; (iii) degradation of aliphatic sulfonates to utilize dimethyl sulfide and methanesulfonate as a carbon and energy and/or sulfur source; (iv) degradation of taurine as an alternative sulfur source for growth in the absence of sulfate; (v) degradation and metabolism of quercetin and other plant flavonoids. The genome sequence also revealed genes involved in degradation of carnitine to trimethylamine (TMA) and malic semialdehyde, which are absent in *K. grimontii* Tre-B. Thus, while *K. grimontii* Tre-B appears to be able to produce TMA through the catabolism of choline in the *cut* BMC, *C. braakii* Tre-T can produce TMA through the catabolism of carnitine.

Effect of PFOA on the antibiotic resistance genes

Whole genome sequencing of *K. grimontii* Tre-B and *C. braakii* Tre-T revealed the presence of numerous resistance genes, in particular to fluoroquinolone antibiotics (Table 3). Therefore, a disk diffusion method experiment was performed to measure the antibiotic susceptibility of Tre-B and Tre-T strains in the MH agar supplemented with increasing concentrations of PFOA (2 $\mu g\ mL^{-1}$, 20 $\mu g\ mL^{-1}$, 200 $\mu g\ mL^{-1}$, 2 mg mL^{-1}) or isopropanol as a control (Fig. 9A).

A slight increase in sensitivity to ampicillin (AMP10) was observed in *C. braakii* Tre-T at a PFOA concentration of 2 mg mL^{-1} (Fig. 9A). In both strains, no appreciable effect in sensitivity to cephalosporins (ceftazidime [CAZ] and cefepime [CFP]), tetracycline (TE) and trimethoprim–sulfamethoxazole (SXT) was detected (Fig. 9A and Table S7†). In contrast, increased resistance to aminoglycosides (amikacin [AK] and tobramycin [TOB]), pefloxacin (PEF), piperacillin (PI), and azithromycin (AZM) was observed in both strains, with resistance levels

Table 6 Pathways for degradation of aromatic compounds and recalcitrant chemicals as inferred from *K. grimontii* Tre-B genome sequence

Locustag	CDS length (bp)	Gene	Product	Pathway
OKNGJBID00372	639	*rutR*	HTH-type transcriptional regulator RutR	Degradation of exogenous pyrimidines as the sole nitrogen source
OKNGJBID00373	1092	*rutA*	Pyrimidine monooxygenase RutA	
OKNGJBID00374	711	*rutB1*	Peroxyureidoacrylate/ ureidoacrylate amidohydrolase RutB	
OKNGJBID00375	393	*rutC1*	Putative aminoacrylate peracid reductase RutC	
OKNGJBID00376	804	*rutD*	Putative aminoacrylate hydrolase RutD	
OKNGJBID00377	591	*rutE*	Putative malonic semialdehyde reductase RutE	
OKNGJBID00378	495	*rutF*	FMN reductase (NADH) RutF	
OKNGJBID00379	1323	*rutG*	Putative pyrimidine permease RutG	
OKNGJBID00754	633	*hpcE1*	Homoprotocatechuate catabolism bifunctional isomerase/decarboxylase	Degradation of homo-protocatechuate
OKNGJBID00755	765	*hpcE2*	Homoprotocatechuate catabolism bifunctional isomerase/decarboxylase	
OKNGJBID00756	1467	*betB1*	NAD/NADP-dependent betaine aldehyde dehydrogenase	
OKNGJBID00757	858	*hpcB*	3,4-Dihydroxyphenylacetate 2,3-dioxygenase	
OKNGJBID00758	381	*hpcD*	5-Carboxymethyl-2-hydroxymuconate delta-isomerase	
OKNGJBID00759	804	*hpcG*	2-Oxo-hept-4-ene-1,7-dioate hydratase	
OKNGJBID00760	792	*hpcH*	4-Hydroxy-2-oxo-heptane-1,7-dioate aldolase	
OKNGJBID00763	1563	*hpaB*	4-Hydroxyphenylacetate 3-monooxygenase oxygenase component	Degradation of 4-hydroxyphenylacetate
OKNGJBID00764	513	*hpaC*	4-Hydroxyphenylacetate 3-monooxygenase reductase component	
OKNGJBID03120	1017	*benC*	Benzoate 1,2-dioxygenase electron transfer component	Degradation of benzoate and 2-halo (F, Br, Cl, I)-benzoate to catechol
OKNGJBID03121	486	*cbdB*	2-Halobenzoate 1,2-dioxygenase small subunit	
OKNGJBID03122	1383	*cbdA*	2-Halobenzoate 1,2-dioxygenase large subunit	
OKNGJBID03123	927	*catA*	Catechol 1,2-dioxygenase	Degradation of catechol to beta-ketoadipate
OKNGJBID03124	291	*catC*	Muconolactone delta-isomerase	
OKNGJBID03125	1119	*catB*	Muconate cycloisomerase 1	
OKNGJBID05375	768	*catD*	3-Oxoadipate enol-lactonase 2	
OKNGJBID03126	798	*pcaR1*	Pca regulon regulatory protein	Degradation of protocatechuate to beta-ketoadipate
OKNGJBID05370	807	*pcaR2*	Pca regulon regulatory protein	
OKNGJBID05374	1353	*pcaB*	3-Carboxy-*cis*,*cis*-muconate cycloisomerase	
OKNGJBID03206	741	*pcaH*	Protocatechuate 3,4-dioxygenase beta chain	
OKNGJBID03207	621	*pcaG*	Protocatechuate 3,4-dioxygenase alpha chain	

© 2025 The Author(s). Published by the Royal Society of Chemistry

Environ. Sci.: Adv., 2025, **4**, 1444–1476 | **1463**

Table 6   (Contd.)

Locustag	CDS length (bp)	Gene	Product	Pathway
OKNGJBID05371	687	pcaI	3-Oxoadipate CoA-transferase subunit A	Degradation of beta-ketoadipate to succinyl-CoA and acetyl-CoA
OKNGJBID05372	657	pcaJ	3-Oxoadipate CoA-transferase subunit B	
OKNGJBID05373	1203	pcaF	Beta-ketoadipyl-CoA thiolase	
OKNGJBID00725	1185	pobA	p-Hydroxybenzoate hydroxylase	Degradation of 4-hydroxybenzoate to protocatechuate
OKNGJBID01380	1194	mhbM	3-Hydroxybenzoate 6-hydroxylase	Degradation of 3-hydroxybenzoate via gentisate to pyruvate and fumarate
OKNGJBID01381	645	nagL	Maleylpyruvate isomerase	
OKNGJBID01382	642	nagK1	Fumarylpyruvate hydrolase	
OKNGJBID01383	1038	nagI	Gentisate 1,2-dioxygenase	
OKNGJBID01384	1359	mhbT	3-Hydroxybenzoate transporter MhbT	
OKNGJBID05070	1353	ntaA	Nitrilotriacetate monooxygenase component A	Degradation of nitrilotriacetate (NTA) to iminodiacetate and glyoxylate
OKNGJBID04245	942	ssuA1	Putative aliphatic sulfonates-binding protein	Degradation of aliphatic sulfonates (dimethyl sulfide, and methanesulfonate)
OKNGJBID04246	1407	dmoA	Dimethyl-sulfide monooxygenase	
OKNGJBID04247	1398		Hypothetical protein	
OKNGJBID04248	1173	ssuD1 (msuD1)	Methanesulfonate monooxygenase	
OKNGJBID00548	576	ssuE	FMN reductase (NADPH)	
OKNGJBID00549	792	ssuC1	Putative aliphatic sulfonates transport permease protein SsuC	
OKNGJBID00550	774	ssuB1	Aliphatic sulfonates import ATP-binding protein SsuB	
OKNGJBID05215	597		3-Mercaptopropionate dioxygenase	
OKNGJBID05216	894	gltC8	HTH-type transcriptional regulator GltC	
OKNGJBID05217	1086	ssuD2 (msuD2)	Methanesulfonate monooxygenase	
OKNGJBID05218	1146	ydbM	Putative acyl-CoA dehydrogenase YdbM	
OKNGJBID05219	975	ssuA2	Putative aliphatic sulfonates-binding protein	
OKNGJBID05220	1038		Hypothetical protein	
OKNGJBID05221	996		Hypothetical protein	
OKNGJBID05222	789	ssuB4	Aliphatic sulfonates import ATP-binding protein SsuB	
OKNGJBID05270	1224	sfnC	Putative FMNH2-dependent monooxygenase SfnC	
OKNGJBID01203	852	tauD	Alpha-ketoglutarate-dependent taurine dioxygenase	Degradation of taurine as an alternative sulfur source for growth in the absence of sulfate
OKNGJBID01204	828	tauC (ssuC2)	Putative aliphatic sulfonates transport permease protein SsuC	
OKNGJBID01205	771	tauB	Taurine import ATP-binding protein TauB	
OKNGJBID01206	963	tauA	Taurine-binding periplasmic protein	
OKNGJBID03899	1038	yhhX	Putative oxidoreductase YhhX	Degradation and metabolism of quercetin
OKNGJBID03900	696	yhhW	Quercetin 2,3-dioxygenase	
OKNGJBID05206	1668	mhpA	3-(3-Hydroxy-phenyl)propionate/3-	

Table 6 (Contd.)

Locustag	CDS length (bp)	Gene	Product	Pathway
			hydroxycinnamic acid hydroxylase	
OKNGJBID05207	945	mhpB	2,3-Dihydroxyphenylpropionate/2,3-dihydroxycinnamic acid 1,2-dioxygenase	
OKNGJBID05208	867	mhpC	2-Hydroxy-6-oxononadienedioate/2-hydroxy-6-oxononatrienedioate hydrolase	
OKNGJBID05209	807	mhpD	2-Keto-4-pentenoate hydratase	
OKNGJBID05210	951	mhpF	Acetaldehyde dehydrogenase	
OKNGJBID05211	1017	mhpE	4-Hydroxy-2-oxovalerate aldolase	
OKNGJBID05212	1197	mhpT	3-(3-Hydroxy-phenyl) propionate transporter	
OKNGJBID03825	873	ectD	Ectoine dioxygenase	Glycine, serine and threonine metabolism
OKNGJBID04586	792	ygiD	4,5-DOPA dioxygenase extradiol	Tyrosine metabolism
OKNGJBID04573	315	ygiN	Putative quinol monooxygenase YgiN	Quinone redox cycle
OKNGJBID03603	306	ydhR	Putative monooxygenase YdhR	
OKNGJBID01443	651	alkB	Alpha-ketoglutarate-dependent dioxygenase AlkB	DNA repair
OKNGJBID02888	1029	vldW1	Validamycin A dioxygenase	Transformation of validamycin A to validamycin B
OKNGJBID04037	1077	vldW2	Validamycin A dioxygenase	
OKNGJBID04040	729	cloR	4-Hydroxy-3-prenylphenylpyruvate oxygenase/4-hydroxy-3-prenylbenzoate synthase	Biosynthesis of secondary metabolites
OKNGJBID03156	1317	moxC	Putative monooxygenase MoxC	Unknown

increasing in parallel with increasing PFOA concentrations, peaking at 2 mg mL^{-1} (Fig. 9A and Table S7†).

An RT-qPCR experiment assessed the transcript levels of five antibiotic resistance-related genes: kpnF, kpnG, adeF, oqxA, and acrA. Strain Tre-B was cultured in LB broth supplemented with PFOA at concentrations of 2, 20, and 200 μg mL^{-1}, and RT-qPCR analysis was subsequently performed to evaluate gene expression levels (Fig. 9B). The results indicate a dose-dependent upregulation of kpnF, kpnG, adeF and oqxA following exposure to increasing concentrations of PFOA (2, 20, and 200 μg mL^{-1}). Expression of acrA was also increased at 20 μg per mL PFOA, but not further at higher PFOA concentrations.

The RT-qPCR results indicate that PFOA activates the transcription of many genes involved in multiple antibiotic resistance in the Tre-B strain, particularly those encoding efflux pumps. The strongest effect was observed at the highest concentration tested (200 μg mL^{-1}), supporting the hypothesis

that PFOA, in addition to select specific groups of bacteria, can enhance antibiotic resistance by upregulating specific ARGs.

Discussion

Although the increase in AMR has been mainly attributed to their misuse or overuse in clinical practice, livestock and agriculture,[103] much remains to be understood about the other drivers of AMR, especially environmental ones. Among the factors involved in the spread of AMR in the environment, the release of large amounts of antibiotics into wastewater and the selective growth of antibiotic-resistant bacteria (ARB) in wastewater treatment plants, and the use of contaminated organic fertilizers and irrigation water in the soils are considered the most relevant.[103,104] However, resistant and multidrug-resistant microbial strains have also been isolated in relatively uninhabited areas of the earth, and there is conclusive evidence that

Environmental Science: Advances

Table 7 Pathways for degradation of aromatic compounds and recalcitrant chemicals as inferred from *C. braakii* Tre-T genome sequence

Locustag	CDS length (bp)	Gene	Product	Pathway
LBFIJIGF02889	1203	*hcaD*	3-Phenylpropionate/cinnamic acid dioxygenase ferredoxin–NAD(+) reductase component	Degradation of 3-phenylpropanoate
LBFIJIGF02890	813	*hcaB*	3-Phenylpropionate-dihydrodiol/cinnamic acid-dihydrodiol dehydrogenase	
LBFIJIGF02891	321	*hcaC*	3-Phenylpropionate/cinnamic acid dioxygenase ferredoxin subunit	
LBFIJIGF02892	519	*hcaF*	3-Phenylpropionate/cinnamic acid dioxygenase subunit beta	
LBFIJIGF02893	1362	*hcaE*	3-Phenylpropionate/cinnamic acid dioxygenase subunit alpha	
LBFIJIGF02894	882	*hcaR*	Hca operon transcriptional activator HcaR	
LBFIJIGF03255	1359	*mhbT*	3-Hydroxybenzoate transporter MhbT	Degradation of 3-hydroxybenzoate *via* gentisate to pyruvate and fumarate
LBFIJIGF03256	1038	*nagI* (*sdgD*)	Gentisate 1,2-dioxygenase	
LBFIJIGF03257	702	*nagK1*	Fumarylpyruvate hydrolase	
LBFIJIGF03258	645	*nagL*	Maleylpyruvate isomerase	
LBFIJIGF03259	1194	*mhbM*	3-Hydroxybenzoate 6-hydroxylase	
LBFIJIGF04525	576	*ssuE*	FMN reductase (NADPH)	Degradation of aliphatic sulfonates (dimethyl sulfide and methanesulfonate)
LBFIJIGF04526	975	*ssuA*	Putative aliphatic sulfonates-binding protein	
LBFIJIGF04527	1146	*ssuD*	Alkanesulfonate monooxygenase	
LBFIJIGF04528	792	*ssuC2*	Putative aliphatic sulfonates transport permease protein SsuC	
LBFIJIGF04529	768	*ssuB*	Aliphatic sulfonates import ATP-binding protein SsuB	
LBFIJIGF00719	852	*tauD1*	Alpha-ketoglutarate-dependent taurine dioxygenase	Degradation of taurine as an alternative sulfur source for growth in the absence of sulfate
LBFIJIGF00720	831	*tauC* (*ssuC1*)	Putative aliphatic sulfonates transport permease protein SsuC	
LBFIJIGF00721	768	*tauB*	Taurine import ATP-binding protein TauB	
LBFIJIGF00722	747	*tauA1*	Taurine-binding periplasmic protein	
LBFIJIGF00723	165	*tauA2*	Taurine-binding periplasmic protein	
LBFIJIGF01999	852	*tauD2*	Alpha-ketoglutarate-dependent taurine dioxygenase	
LBFIJIGF00372	1038	*yhhX*	Putative oxidoreductase YhhX	Degradation and metabolism of quercetin
LBFIJIGF00373	696	*yhhW*	Quercetin 2,3-dioxygenase	
LBFIJIGF00732	1212	*mhpT*	3-(3-Hydroxy-phenyl)propionate transporter	
LBFIJIGF00733	1014	*mhpE*	4-Hydroxy-2-oxovalerate aldolase	
LBFIJIGF00734	951	*mhpF*	Acetaldehyde dehydrogenase	
LBFIJIGF00735	810	*mhpD*	2-Keto-4-pentenoate hydratase	
LBFIJIGF00736	867	*mhpC*	2-Hydroxy-6-oxononadienedioate/2-	

Table 7 (Contd.)

Locustag	CDS length (bp)	Gene	Product	Pathway
LBFIJIGF00737	945	mhpB	hydroxy-6-oxononatrienedioate hydrolase 2,3-Dihydroxyphenylpropionate/2,3-dihydroxicinnamic acid 1,2-dioxygenase	
LBFIJIGF00738	1665	mhpA	3-(3-Hydroxy-phenyl) propionate/3-hydroxycinnamic acid hydroxylase	
LBFIJIGF03591	966	yeaX	Carnitine monooxygenase reductase subunit	Degradation of carnitine to trimethylamine and malic semialdehyde
LBFIJIGF03592	1125	yeaW	Carnitine monooxygenase oxygenase subunit	
LBFIJIGF03593	1602	caiT2	L-Carnitine/gamma-butyrobetaine antiporter	
LBFIJIGF02638	789	ygiD	4,5-DOPA dioxygenase extradiol	Tyrosine metabolism
LBFIJIGF02647	315	ygiN	Putative quinol monooxygenase YgiN	Quinone redox cycle
LBFIJIGF04036	309	ydhR	Putative monooxygenase YdhR	
LBFIJIGF03175	651	alkB	Alpha-ketoglutarate-dependent dioxygenase AlkB	DNA repair
LBFIJIGF03867	1314	moxC	Putative monooxygenase MoxC	Unknown
LBFIJIGF00134	306		Putative monooxygenase	Unknown

antibiotic resistance is ancient. A highly diverse collection of genes encoding resistance to β-lactam, tetracycline and glycopeptide antibiotics was recovered by sequencing of ancient DNA recovered from Late Pleistocene permafrost sediments.[105] Furthermore, ARB and antibiotic resistance genes (ARG) were recently detected in minimally human-impacted environments including Antarctica although further research is required for better detecting and quantifying ARB and ARG along human gradients to better characterize the factors leading to their spread in pristine environments.[106,107] Therefore, something is still missing regarding a complete understanding of the environmental drivers of AMR. Understanding the environmental drivers of AMR is critical because the circulation of bacterial ARG in different environments can be considered a potential factor in the transfer of these genes to health centers.[108,109]

In this study, the results of Winogradsky column experiments provided some evidence for a link between PFAS contamination and AMR. While the effects of PFOA and PFOS on soil microbial communities have been extensively explored in observational studies, Winogradsky columns as miniature ecosystem offer the opportunity to analyze, under controlled laboratory conditions, specific effects related to, for example, a single PFAS congener or combination thereof, as well as possible synergistic interactions between PFAS and other environmental contaminants. It also provides an opportunity to analyze PFAS metabolism over time, both in the aerobic and anaerobic zones of the column, microbial successions, transcriptional activity, and specific microbial activities stimulated by the presence of PFAS for computational modeling and pathway prediction, as demonstrated for other environmental pollutants.[110,111] By using this experimental system, it is possible to carry out biostimulation or biological enrichment experiments.

In line with a recent study,[34] here we demonstrate that environmental PFAS contamination may act as a driver for the selection of environmental ARBs that behave as opportunistic pathogens in humans. Microbial communities from the PFAS-contaminated Trelleborg site B1 were stimulated with a high concentration of PFOA in microcosm experiments, and this resulted in the isolation of two bacterial species, K. grimontii and C. braakii that are known to cause opportunistic infections. Both K. grimontii Tre-B and C. braakii Tre-T are characterized by a large set of genes involved in AMR, in particular to fluoroquinolones (Table 3).

Strains of K. grimontii were isolated from human blood cultures, wound infections, antibiotic-associated colitis, as well as from feces of healthy patients.[79] Klebsiella species are commonly found in water, soil and plants and as commensals in the intestine of animals, including humans.[112] There is increasing concern about the environmental spread of these bacteria because they are even more frequently associated with nosocomial infections and are developing multidrug
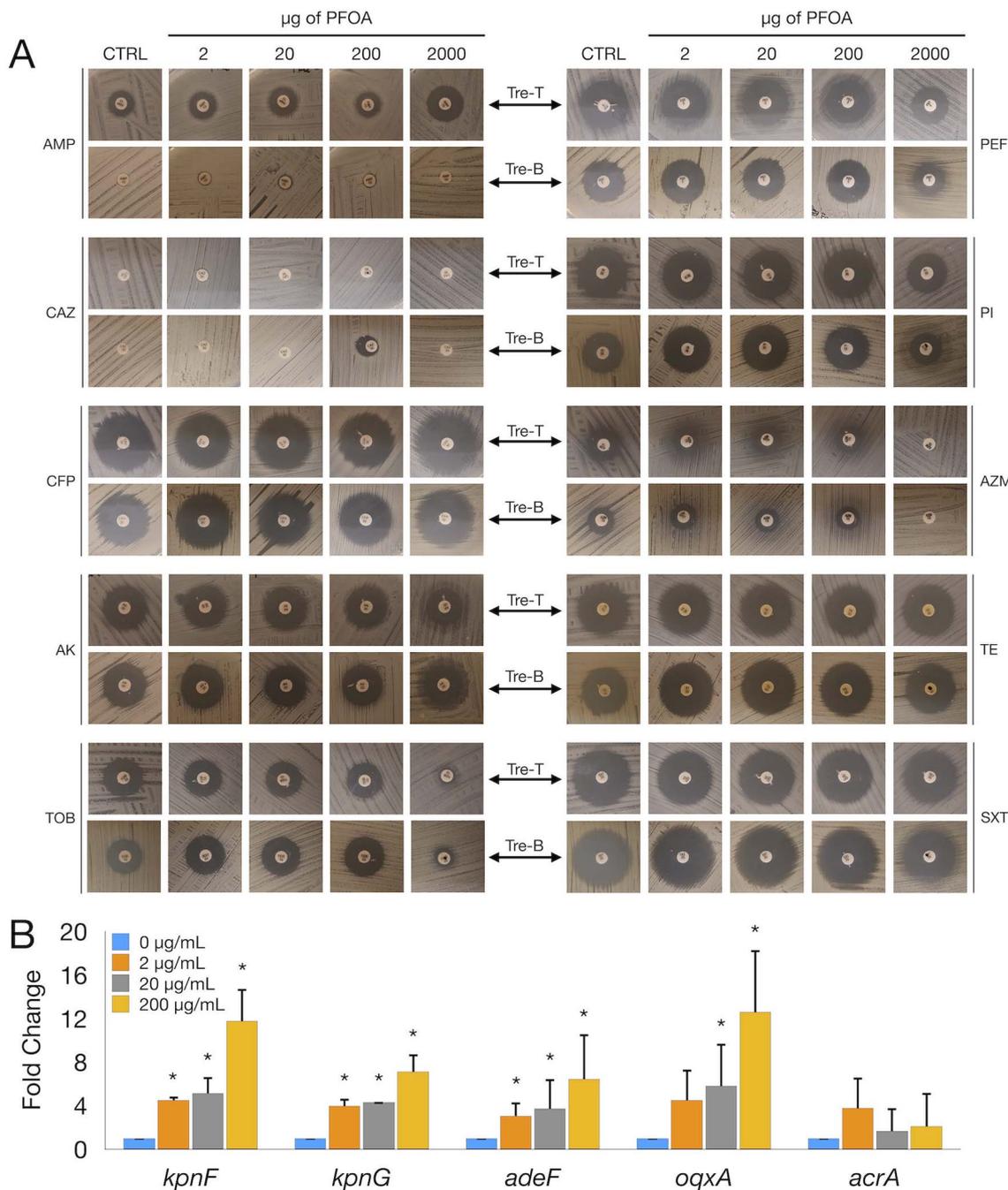
Fig. 9 Impact of PFOA on antibiotic susceptibility testing and transcription levels of antibiotic-resistance genes. (A) Kirby−Bauer test results on Mueller−Hinton (MH) agar for *K. grimontii* Tre-B and *C. braakii* Tre-T. The following antibiotics were used: ampicillin 10 µg (AMP10), cefoperazone 30 µg (CAZ30), ceftazidime 30 µg (CFP30), amikacin 30 µg (AK30), tobramycin 10 µg (TOB10), pefloxacin 5 µg (PEF5), pipemidic acid 20 µg (PI20), azithromycin 15 µg (AZM15), tetracycline 30 µg (TE30), and trimethoprim-sulfamethoxazol 25 µg (SXT25). (B) Levels of transcript (RT-qPCR) of five antibiotic resistance-related genes (*kpnF*, *kpnG*, *adeF*, *oqxA*, and *acrA*) of *K. grimontii* Tre-B grown in LB supplemented with an incremental concentration of PFOA. Asterisks indicate statistical significance (*p*-value <0.05) compared to the control.

resistance.[113] *Klebsiella oxytoca* is the second most common *Klebsiella* species causing disease in humans, after *K. pneumoniae*.[80]

Citrobacter species are commonly found in water, soil and plants and as commensal in the intestine of animals, including humans. Occasionally, they can cause enteric diseases but they

are also associated with extraintestinal disorders, among which the most significant are neonatal meningitis and brain abscesses, and are rarely implicated in skin or soft tissue infections.[114,115] *C. braakii* strains have been described as plant growth-promoting rice rhizobacteria.[116] At the same time, *C. braakii* is a human opportunistic pathogen that has been

implicated in enteric diseases (gastroenteritis), and rarely in sepsis and multiorgan dysfunctions in immunocompromised patients.[117,118] A recent case of bacteremia due to carbapenem-resistant *C. braakii* has been reported.[119]

Although antibiotic resistance is of particular concern in pathogenic bacteria, a growing number of studies draw attention to the worrying increase in the prevalence of AMR in non-pathogenic (commensal) bacterial species of the human microbiota.[120] These commensal bacterial species, including several members of the large family of Enterobacteriaceae, can transfer ARG to pathogenic species and can themselves cause opportunistic infections in humans.[121,122] Furthermore, most of them are environmental species capable of growing or to persisting in different environmental niches and undertaking horizontal gene transfer with other environmental bacteria.[123]

It can be noted that both *K. grimontii* and *C. braakii* belong to family of Enterobacteriaceae (γ-Proteobacteria), consistent with the growing evidence that exposure to PFAS leads to an enrichment of several bacterial phyla, mostly Proteobacteria, which are more resistant to PFAS than other phyla.[18,22,33] Negatively charged outer membrane repelling negatively charged PFAS, an increased ability to cope with oxidative damage and/or DNA damage, or even an ability to extrude PFAS from cells or immobilize these compounds in a biofilm are possible mechanisms of resistance of these Enterobacteriaceae to PFAS.

From a mechanistic point of view, it is crucial to understand the mechanisms by which the presence of PFASs can promote the selection in the environment of bacteria resistant to antibiotics, particularly fluoroquinolones. Fluoroquinolones target type II bacterial topoisomerases and are widely used in the medical, livestock and aquaculture sectors. The presence of fluoroquinolone antibiotics is ubiquitous and poses a serious threat to ecosystems.[124] They are not readily biodegradable and can also accumulate in soils and sediments due to their adsorption properties.

Bacterial resistance to these compounds is due to multiple mechanisms, including mutations in one or more of the genes encoding the primary and secondary targets of these drugs (*gyrA, gyrB, parC, parE*), the type II topoisomerases, permeability changes, such as porin loss in Gram-negative bacteria or up-regulation of chromosomal efflux systems (*patAB, acrAB-tolC*). Transmissible fluoroquinolone-resistance is often associated with the acquirement of plasmid-mediated quinolone resistance (PMQR) genes encoding proteins that prevent binding of fluoroquinolones to type II topoisomerases (*qnrA, qnrB, qnrC, qnrD, qnrS*), degrade (*aac(6')lb-cr*) or extrude (*oqxAB* and *qepA* efflux systems) the fluoroquinolones.[125] Possession of these resistance mechanisms enables the survival of fluoroquinolone-resistant bacteria not only in the infected host, but also in environments contaminated with these antibiotics.

Among the ARGs present in both *K. grimontii* Tre-B and *C. braakii* Tre-T, it can be noted the presence of the genes encoding AcrAB-TolC because this multidrug efflux pump confers resistance to a wide range of toxic compounds such as antibiotics, surfactants, dyes, detergents, and disinfectants which are not found in the natural environment of these bacteria. Moreover, in *C. braakii* Tre-T, Resistance Gene Identifier predicted the

presence of EmrAB-TolC MSF efflux system, structurally similar to AcrAB-TolC, conferring reduced susceptibility to a large variety of unrelated antimicrobial compounds.[126,127] In *K. grimontii* Tre-B the transmissible *oqxAB* efflux system was also found. This system confers reduced susceptibility to a multitude of substrates, including several antibiotics (including quinolones, quinoxalines, tigecycline, nitrofurantoin and chloramphenicol), detergents and disinfectants (benzalkonium chloride, triclosan and sodium dodecyl sulfate).[128,129] Furthermore, in *K. grimontii* Tre-B, Resistance Gene Identifier predicted the presence of the AdeFGH efflux system that was associated with decreased susceptibility to many antibiotics, like chloramphenicol and fluoroquinolones, and a number of compounds, as well as biofilm formation in *Acinetobacter baumannii*.[130,131] Intriguingly, we found by RT-qPCR experiments that the transcript levels of some of these genes (*acrA, adeF,* and *oqxA*) increased when the Tre-B strain was grown in the presence of PFOA. In particular, *adeF* and *oqxA* showed a dose-dependent increase in transcript levels in response to PFOA exposure, whereas *acrA* was upregulated only at low PFOA concentrations. This result suggests that PFOA, in addition to selecting different groups of microorganisms in polluted environments, may enhance antibiotic resistance through upregulation of specific ARGs.

Furthermore, it would be interesting to investigate a possible involvement of these efflux systems in PFAS resistance, to understand if there is a mechanistic connection between these chemicals and antibiotic resistance, particularly to fluoroquinolones. In *K. grimontii* Tre-B, genes encoding the efflux pump KpnGH of the MFS superfamily and KpnEF of the small multidrug resistance (SMR) family were also identified. These systems contribute to reduced susceptibility to a wide range of antibiotics, dyes, detergents and disinfectants.[132,133] In addition, KpnEF, which is also present in *C. braakii* Tre-T, was directly involved in capsule biogenesis in *K. pneumoniae*.[132] Therefore, some of these transport systems, including AdeFGH and KpnEF, could mediate both antimicrobial and PFAS resistance by increasing the production of exopolysaccharides and capsular polysaccharides. This hypothesis could be validated by testing defective mutants in these transport systems. It is also interesting to analyze the expression of these transport systems in response to PFAS exposure. In this regard, it is worth noting that the expression of the efflux pump AcrAB-TolC was significantly up-regulated in *E. coli* strains DH5α and HB101 exposed to PFOA.[134] Consistent with this result, we found by RT-qPCR experiments that the transcript levels of *kpnF, kpnG* and *acrA* genes increased when bacteria were grown with PFOA, and that in the case of *kpnF* and *kpnG* this increase was striking and dependent on PFOA concentrations.

K. grimontii Tre-B and *C. braakii* Tre-T could be useful to further understand the adaptive responses of bacteria to PFAS exposure by transcriptomics studies, as was recently done using model strains of *E. coli*.[134] Notably, in *E. coli*, PFOA has been shown to induce oxidative stress, enhance cell membrane permeability and promote the excretion of extracellular polymeric substances.[134] This latter finding is consistent with our hypothesis that some of these transport systems could mediate

© 2025 The Author(s). Published by the Royal Society of Chemistry

Environ. Sci.: Adv., 2025, **4**, 1444–1476 | **1469**

both antimicrobial and PFAS resistance by increasing the production of extracellular polymers and capsule.

An additional mechanism could be involved in the PFAS/fluoroquinolone cross-resistance in polluted environment: resistance to fluoride. As well as PFAS, fluoroquinolones are characterized by the presence of fluorine atom, which forms an exceptionally strong and highly polarized C–F bond, making them recalcitrant to biodegradation.[135] All biodegradation pathways of these compounds involve their defluorination,[124] with the release of fluoride, a very toxic compound to microorganisms.[26] Fluoride is detrimental to biological systems mainly because of enzyme inhibition. The electronegative F^- effectively outcompetes electronegative substrate groups, such as OH^-, phosphate, or carboxylate, for coordination by an enzyme-bound metal ion causing broad-spectrum harm to many metabolic pathways.[136,137] To survive in fluoroquinolone-contaminated environments, fluoroquinolone-resistant bacteria must have the ability to resist toxic fluoride. Fluoride is also released as a consequence of PFAS defluorination, and is another important factor in determining PFAS resistance.

Among the mechanisms of resistance to fluoride that some microorganisms have evolved is the export of fluoride via the CLC^F family of F^-/H^+ antiporters.[26] We found in both *K. grimontii* Tre-B and *C. braakii* Tre-T the gene coding for fluoride ion transport (*crcB*) (Fig. 8). This gene is localized in a conserved chromosome region and co-occurs in Enterobacteriaceae with genes involved in the biosynthesis of lipoic acid from octanoic acid, as well as with genes involved in sulfur metabolism and oxidative stress (Fig. 8), and it may be noted that in rat α-lipoic acid alleviate fluoride-induced damage to liver.[138] α-Lipoic acid, a natural free radical scavenger, alleviated fluoride-induced iron accumulation, increased oxidative stress, and elevated lipid peroxidation in the liver. Therefore, this gene locus could be involved in fluoride detoxification, contributing to the ability of these bacteria to survive in environments polluted by PFAS and/or fluoroquinolones. It might be interesting to analyze the expression of this fluoride ion transport in response to PFAS exposure.

In the same chromosome region, it may be also noted the presence of two genes encoding specific and distinct oxidases in the two bacteria: *dsmA2* in *K. grimontii* Tre-B coding for a dimethyl sulfoxide/trimethylamine *N*-oxide reductase, and *ynfE1* in *C. braakii* Tre-T coding for a putative dimethyl sulfoxide reductase. Indeed, both bacteria were able to grow anaerobically using dimethyl sulfoxide as terminal electron acceptor. Furthermore, potential trimethylamine *N*-oxide reductase activity in *K. grimontii* Tre-B is of particular interest because of the presence of the *cut* BMC locus in the genome of this microorganism.

A characteristic of the *K. grimontii* Tre-B genome is the presence of a resistance plasmid (named pKGTreB) containing many genes involved in resistance to arsenic, copper, mercury and silver (Table 5). Especially the availability of information on a silver resistance plasmid is useful due to the widespread antimicrobial use of silver ions and nanoparticles against bacteria, fungi and viruses and the need to gain further knowledge on silver ion and toxicity mechanisms and

nanoparticles.[139] Furthermore, the observed cross-resistance between resistance to silver and resistance to other heavy metals and antibiotics in bacteria is also a clinically and environmentally important issue.

Another feature of the *K. grimontii* Tre-B genome is the presence of a large set of genes involved in the degradation of aromatic compounds, including halogenated ones, and other recalcitrant chemicals (Table 6). Many of these genes are also present in the genome of *C. braakii* Tre-T (Table 7), including those involved in the degradation of aliphatic sulfonates (dimethylsulfide and methanesulfonate). The presence of the latter genes may be related to the fact that the Trelleborg site has long been used industrially for production of tires, and it is known that the rubber vulcanization process involves the addition of a mixture of sulfur and other additives, whose release into the environment may have acted as a selection factor for local microbial communities.

Given the genomic and metabolic complexity of these bacteria, the selection of antibiotic-resistant strains observed in our study may be influenced by interactions between PFAS and other co-contaminants. As reported in previous studies, such interactions can facilitate the uptake, transport, and release of PFAS.[74–76] Consequently, further research is needed to investigate these dynamics in both polluted environments, such as the Trelleborg landfill, and natural settings. Moreover, the microcosm and RT-qPCR experiments were conducted using only PFOA. Additional studies are therefore necessary to assess the effects of other PFAS compounds.

Conclusion

Microbial communities are fundamental to maintaining ecosystem health by driving key biogeochemical cycles, including carbon, nitrogen, sulfur, and phosphorus cycles. Disruptions to these communities, such as those caused by PFAS contamination, can have significant consequences for microbial-mediated processes like nutrient cycling, organic matter decomposition, and pollutant degradation. In PFAS-contaminated environments, the altered community structure—characterized by the dominance of PFAS-resistant strains such as *Klebsiella grimontii* and *Citrobacter braakii*—signals a shift toward microbial populations that thrive under high levels of environmental stress.

The enrichment of antibiotic-resistant bacteria (ARB) in these ecosystems raises concerns about the broader impacts on ecosystem function. This shift may suppress sensitive but ecologically vital microbial species responsible for nutrient cycling and soil health, leading to potential imbalances in nutrient availability and ecosystem productivity. For example, nutrient-poor soils could affect plant growth and disrupt higher trophic levels, ultimately altering the structure of entire ecosystems.

Furthermore, the accumulation of antibiotic-resistant pathogens in PFAS-contaminated environments may have cascading effects throughout the food web. Wildlife exposed to contaminated water or prey may face physiological and reproductive risks from both PFAS and ARB exposure. The bioaccumulation

1470 | *Environ. Sci.: Adv.*, 2025, **4**, 1444–1476

© 2025 The Author(s). Published by the Royal Society of Chemistry

of PFAS, compounded by the spread of resistance genes *via* horizontal gene transfer, could exacerbate these effects, increasing the spread of multidrug resistance (MDR) within natural populations. The simultaneous exposure to chemical pollutants and resistant microbes creates a dual burden on wildlife and ecosystems, complicating efforts to maintain biodiversity and ecosystem resilience.

The ability of *K. grimontii* and *C. braakii* to resist both antibiotics and environmental pollutants suggests that these bacteria could act as vectors for the spread of multidrug resistance through soils, sediments, and aquatic systems. The transfer of resistance genes to other pathogenic or opportunistic bacteria *via* horizontal gene transfer increases the risk of AMR beyond the immediate contaminated sites. This has broad implications for public health, as the global AMR crisis continues to be exacerbated by the spread of environmental resistance, posing challenges for both animal and human health.

These findings highlight the urgent need for comprehensive environmental policies that address not only the chemical toxicity of PFAS but also their role in promoting antimicrobial resistance. Current regulatory frameworks focus largely on chemical contaminants, with less attention to their ecological consequences. Expanding these frameworks to include microbial community monitoring in PFAS-contaminated sites could provide a more holistic assessment of the long-term environmental and health risks posed by these pollutants. Such policies would better account for the complex interactions between chemical and biological factors that drive resistance and ecosystem disruption.

Data availability

Sequencing data for this article are available under the following accession numbers: PRJEB89934. The other data supporting this article have been included as part of the ESI.†

Author contributions

Conceptualization: PA, FD; data curation: MC, MT, AG, DG, DR, CL, AR; formal analysis: MC, AC, AG, CL, AR, MM, KEK; funding acquisition: FD, PA; investigation: MC, PA, FD, AC, CL, KEK; methodology: PA, MC, MT; project administration: PA, FD; resources: KEK, FD, DR, DG; visualization: MC, AG; supervision: PA, FD; writing – original draft: PA, MC, FD, CL; writing – review & editing: PA, MC, FD, CL, AC, AR.

Conflicts of interest

There are no conflicts to declare.

Acknowledgements

References

1 C. F. Kwiatkowski, D. Q. Andrews, L. S. Birnbaum, T. A. Bruton, J. C. DeWitt, D. R. U. Knappe, M. V. Maffini, M. F. Miller, K. E. Pelch, A. Reade, A. Soehl, X. Trier, M. Venier, C. C. Wagner, Z. Wang and A. Blum, Scientific Basis for Managing PFAS as a Chemical Class, *Environ. Sci. Technol. Lett.*, 2020, **7**, 532–543.

2 J. Glüge, M. Scheringer, I. T. Cousins, J. C. DeWitt, G. Goldenman, D. Herzke, R. Lohmann, C. A. Ng, X. Trier and Z. Wang, An overview of the uses of per- and polyfluoroalkyl substances (PFAS), *Environ. Sci.: Processes Impacts*, 2020, **22**, 2345–2373.

3 R. Renner, Growing Concern Over Perfluorinated Chemicals, *Environ. Sci. Technol.*, 2001, **35**, 154A–160A.

4 C. Lau, K. Anitole, C. Hodes, D. Lai, A. Pfahles-Hutchens and J. Seed, Perfluoroalkyl Acids: A Review of Monitoring and Toxicological Findings, *Toxicol. Sci.*, 2007, **99**, 366–394.

5 A. M. Seacat, Subchronic Toxicity Studies on Perfluorooctanesulfonate Potassium Salt in Cynomolgus Monkeys, *Toxicol. Sci.*, 2002, **68**, 249–264.

6 V. Ehrlich, W. Bil, R. Vandebriel, B. Granum, M. Luijten, B. Lindeman, P. Grandjean, A.-M. Kaiser, I. Hauzenberger, C. Hartmann, C. Gundacker and M. Uhl, Consideration of pathways for immunotoxicity of per- and polyfluoroalkyl substances (PFAS), *Environ. Health*, 2023, **22**, 19.

7 M. N. Ehsan, M. Riza, M. N. Pervez, M. M. O. Khyum, Y. Liang and V. Naddeo, Environmental and health impacts of PFAS: Sources, distribution and sustainable management in North Carolina (USA), *Sci. Total Environ.*, 2023, **878**, 163123.

8 G. L. Kennedy, J. L. Butenhoff, G. W. Olsen, J. C. O'Connor, A. M. Seacat, R. G. Perkins, L. B. Biegel, S. R. Murphy and D. G. Farrar, The Toxicology of Perfluorooctanoate, *Crit. Rev. Toxicol.*, 2004, **34**, 351–384.

9 U. M. Ismail, H. Elnakar and M. F. Khan, Sources, Fate, and Detection of Dust-Associated Perfluoroalkyl and Polyfluoroalkyl Substances (PFAS): A Review, *Toxics*, 2023, **11**, 335.

10 C. Lau, J. L. Butenhoff and J. M. Rogers, The developmental toxicity of perfluoroalkyl acids and their derivatives, *Toxicol. Appl. Pharmacol.*, 2004, **198**, 231–241.

11 Y. Manojkumar, S. Pilli, P. V. Rao and R. D. Tyagi, Sources, occurrence and toxic effects of emerging per- and polyfluoroalkyl substances (PFAS), *Neurotoxicol. Teratol.*, 2023, **97**, 107174.

12 J. Sun, L. Xing and J. Chu, Global ocean contamination of per- and polyfluoroalkyl substances: A review of seabird exposure, *Chemosphere*, 2023, **330**, 138721.

13 Z. Sun, Y. Wen, B. Wang, S. Deng, F. Zhang, Z. Fu, Y. Yuan and D. Zhang, Toxic effects of per- and polyfluoroalkyl substances on sperm: Epidemiological and experimental evidence, *Front. Endocrinol.*, 2023, **14**, 1114463.

14 Z.-J. Wen, Y.-J. Wei, Y.-F. Zhang and Y.-F. Zhang, A review of cardiovascular effects and underlying mechanisms of

legacy and emerging per- and polyfluoroalkyl substances (PFAS), *Arch. Toxicol.*, 2023, **97**, 1195–1245.

15 X. Zhang, J. A. Flaws, M. J. Spinella and J. Irudayaraj, The Relationship between Typical Environmental Endocrine Disruptors and Kidney Disease, *Toxics*, 2022, **11**, 32.

16 The Forever Pollution Project – Journalists tracking PFAS across Europe, https://foreverpollution.eu/, accessed 17 September 2024.

17 S. Huang and P. R. Jaffé, Defluorination of Perfluorooctanoic Acid (PFOA) and Perfluorooctane Sulfonate (PFOS) by *Acidimicrobium* sp. Strain A6, *Environ. Sci. Technol.*, 2019, **53**, 11410–11419.

18 Y. Bao, B. Li, S. Xie and J. Huang, Vertical profiles of microbial communities in perfluoroalkyl substance-contaminated soils, *Ann. Microbiol.*, 2018, **68**, 399–408.

19 Y. Ke, J. Chen, X. Hu, T. Tong, J. Huang and S. Xie, Emerging perfluoroalkyl substance impacts soil microbial community and ammonia oxidation, *Environ. Pollut.*, 2020, **257**, 113615.

20 Y. Sun, T. Wang, X. Peng, P. Wang and Y. Lu, Bacterial community compositions in sediment polluted by perfluoroalkyl acids (PFAAs) using Illumina high-throughput sequencing, *Environ. Sci. Pollut. Res.*, 2016, **23**, 10556–10565.

21 M. Sun, E. Arevalo, M. Strynar, A. Lindstrom, M. Richardson, B. Kearns, A. Pickett, C. Smith and D. R. U. Knappe, Legacy and Emerging Perfluoroalkyl Substances Are Important Drinking Water Contaminants in the Cape Fear River Watershed of North Carolina, *Environ. Sci. Technol. Lett.*, 2016, **3**, 415–419.

22 W. Qiao, Z. Xie, Y. Zhang, X. Liu, S. Xie, J. Huang and L. Yu, Perfluoroalkyl substances (PFASs) influence the structure and function of soil bacterial community: Greenhouse experiment, *Sci. Total Environ.*, 2018, **642**, 1118–1126.

23 D. Zhang, W. Zhang and Y. Liang, Distribution of eight perfluoroalkyl acids in plant-soil-water systems and their effect on the soil microbial community, *Sci. Total Environ.*, 2019, **697**, 134146.

24 D. Zhang, W. Zhang and Y. Liang, Bacterial community in a freshwater pond responding to the presence of perfluorooctanoic acid (PFOA), *Environ. Technol.*, 2020, **41**, 3646–3656.

25 L. P. Wackett, Nothing lasts forever: understanding microbial biodegradation of polyfluorinated compounds and perfluorinated alkyl substances, *Microb. Biotechnol.*, 2022, **15**, 773–792.

26 B. C. McIlwain, M. T. Ruprecht and R. B. Stockbridge, Membrane Exporters of Fluoride Ion, *Annu. Rev. Biochem.*, 2021, **90**, 559–579.

27 E. Shahsavari, D. Rouch, L. S. Khudur, D. Thomas, A. Aburto-Medina and A. S. Ball, Challenges and Current Status of the Biological Treatment of PFAS-Contaminated Soils, *Front. Bioeng. Biotechnol.*, 2021, **8**, 602040.

28 L. Philippot, C. Chenu, A. Kappler, M. C. Rillig and N. Fierer, The interplay between microbial communities and soil properties, *Nat. Rev. Microbiol.*, 2024, **22**, 226–239.

29 P. Liu, S. Wen, S. Zhu, X. Hu and Y. Wang, Microbial Degradation of Soil Organic Pollutants: Mechanisms, Challenges, and Advances in Forest Ecosystem Management, *Processes*, 2025, **13**, 916.

30 D. V. Murphy, E. A. Stockdale, P. C. Brookes and K. W. T. Goulding, in *Soil Biological Fertility*, ed. L. K. Abbott and D. V. Murphy, Springer Netherlands, Dordrecht, 2004, pp. 37–59.

31 W. Qiao, Z. Xie, Y. Zhang, X. Liu, S. Xie, J. Huang and L. Yu, Perfluoroalkyl substances (PFASs) influence the structure and function of soil bacterial community: Greenhouse experiment, *Sci. Total Environ.*, 2018, **642**, 1118–1126.

32 S. N. Davis, S. M. Klumker, A. A. Mitchell, M. A. Coppage, J. M. Labonté and A. Quigg, Life in the PFAS lane: The impact of perfluoroalkyl substances on photosynthesis, cellular exudates, nutrient cycling, and composition of a marine microbial community, *Sci. Total Environ.*, 2024, **927**, 171977.

33 Y. Cai, H. Chen, R. Yuan, F. Wang, Z. Chen and B. Zhou, Metagenomic analysis of soil microbial community under PFOA and PFOS stress, *Environ. Res.*, 2020, **188**, 109838.

34 C. Chen, Y. Fang, X. Cui and D. Zhou, Effects of trace PFOA on microbial community and metabolisms: Microbial selectivity, regulations and risks, *Water Res.*, 2022, **226**, 119273.

35 C. Liu, X. Zhu, L. You, K. Y.-H. Gin, H. Chen and B. Chen, Per/polyfluoroalkyl substances modulate plasmid transfer of antibiotic resistance genes: A balance between oxidative stress and energy support, *Water Res.*, 2023, **240**, 120086.

36 Z. Xu, J. Xiong, C. Li, S. Hu, Z. Li, Y. Ma, S. Li, B. Huang, X. Ren and X. Pan, Environmental concentrations of per/polyfluoroalkyl substances promote the conjugative transfer of antibiotic resistance genes, *Chem. Eng. J.*, 2024, **498**, 155500.

37 Y. Li, Y. Zhang, X. Liu, X. Zhou, T. Ye, Q. Fu, M. Du, Q. Lu, Y. Zheng and D. Wang, Per- and polyfluoroalkyl substances exacerbate the prevalence of plasmid-borne antibiotic resistance genes by enhancing natural transformation, in vivo stability, and expression in bacteria, *Water Res.*, 2025, **272**, 122972.

38 E. Abbasi Montazeri, A. D. Khosravi, M. Saki, M. Sirous, B. Keikhaei and S. Seyed-Mohammadi, Prevalence of Extended-Spectrum Beta-Lactamase-Producing Enterobacteriaceae Causing Bloodstream Infections in Cancer Patients from Southwest of Iran, *Infect. Drug Resist.*, 2020, **13**, 1319–1326.

39 A. Farajzadeh Sheikh, M. Moradi Bandbal and M. Saki, Emergence of multidrug-resistant *Shigella* species harboring extended-spectrum beta-lactamase genes in pediatric patients with diarrhea from southwest of Iran, *Mol. Biol. Rep.*, 2020, **47**, 7097–7106.

40 K. Garbacz, M. Wierzbowska, E. Kwapisz, M. Kosecka-Strojek, M. Bronk, M. Saki and J. Międzobrodzki, Distribution and antibiotic-resistance of different *Staphylococcus* species identified by matrix assisted laser desorption ionization-time of flight mass spectrometry

(MALDI-TOF MS) isolated from the oral cavity, *J. Oral Microbiol.*, 2021, **13**, 1983322.

41 WHO, Antimicrobial resistance, https://www.who.int/health-topics/antimicrobial-resistance, accessed 13 June 2023.

42 EU, EU Action on Antimicrobial Resistance, European Commission, https://health.ec.europa.eu/antimicrobial-resistance/eu-action-antimicrobial-resistance_en, accessed 13 June 2023.

43 Council of The European Union, *Council Recommendation on Stepping up EU Actions to Combat Antimicrobial Resistance in a One Health Approach 2023/C 220/01*, 2023.

44 J. O'Neill and Grande-Bretagne, *Antimicrobial Resistance: Tackling a Crisis for the Health and Wealth of Nations, Review on Antimicrobial Resistance*, 2014.

45 J. O'Neill, *Tackling Drug-Resistant Infections Globally: Final Report and Recommendations*, Government of the United Kingdom, 2016.

46 NOAH, NOAH responds to the O'Neill review, ProQuest, https://www.proquest.com/docview/1809928859?parentSessionId=fiAy%2Bi4DqmXU9DIR5m2Y5VVWdf1bVCKLk9MLOJc3xPM%3D&sourcetype=ScholarlyJournals, accessed 16 September 2024.

47 M. Gao, Q. Zhang, C. Lei, T. Lu and H. Qian, Atmospheric antibiotic resistome driven by air pollutants, *Sci. Total Environ.*, 2023, **902**, 165942.

48 A. H. Holmes, L. S. P. Moore, A. Sundsfjord, M. Steinbakk, S. Regmi, A. Karkey, P. J. Guerin and L. J. V. Piddock, Understanding the mechanisms and drivers of antimicrobial resistance, *Lancet*, 2016, **387**, 176–187.

49 R. Magnano San Lio, G. Favara, A. Maugeri, M. Barchitta and A. Agodi, How Antimicrobial Resistance Is Linked to Climate Change: An Overview of Two Intertwined Global Challenges, *Int. J. Environ. Res. Publ. Health*, 2023, **20**, 1681.

50 G. Pizzolante, C. Cordero, S. M. Tredici, D. Vergara, P. Pontieri, L. Del Giudice, A. Capuzzo, P. Rubiolo, C. N. Kanchiswamy, S. A. Zebelo, C. Bicchi, M. E. Maffei and P. Alifano, Cultivable gut bacteria provide a pathway for adaptation of *Chrysolina herbacea* to *Mentha aquatica* volatiles, *BMC Plant Biol.*, 2017, **17**, 30.

51 M. Calcagnile, I. Jeguirim, S. M. Tredici, F. Damiano and P. Alifano, Spiramycin Disarms *Pseudomonas aeruginosa* without Inhibiting Growth, *Antibiotics*, 2023, **12**, 499.

52 E. P. Goldschmidt, M. S. Cater, T. S. Matney, M. Ann Butler and A. Greene, Genetic Analysis Of The Histidine Operon In *Escherichia Coli* K12, *Genetics*, 1970, **66**, 219–229.

53 T. Kasai, Regulation of the expression of the histidine operon in *Salmonella typhimurium*, *Nature*, 1974, **249**, 523–527.

54 D. Vinella and R. D'Ari, Thermoinducible filamentation in *Escherichia coli* due to an altered RNA polymerase beta subunit is suppressed by high levels of ppGpp, *J. Bacteriol.*, 1994, **176**, 966–972.

55 A. Talà, M. Calcagnile, S. C. Resta, A. Pennetta, G. E. De Benedetto and P. Alifano, Thiostrepton, a resurging drug inhibiting the stringent response to counteract antibiotic-resistance and expression of virulence determinants in *Neisseria gonorrhoeae*, *Front. Microbiol.*, 2023, **14**, 1104454.

56 A. Talà, A. Buccolieri, M. Calcagnile, G. Ciccarese, M. Onorato, R. Onorato, A. Serra, F. Spedicato, S. M. Tredici, P. Alifano and G. Belmonte, Chemotrophic profiling of prokaryotic communities thriving on organic and mineral nutrients in a submerged coastal cave, *Sci. Total Environ.*, 2021, **755**, 142514.

57 T. Z. DeSantis, P. Hugenholtz, N. Larsen, M. Rojas, E. L. Brodie, K. Keller, T. Huber, D. Dalevi, P. Hu and G. L. Andersen, Greengenes, a Chimera-Checked 16S rRNA Gene Database and Workbench Compatible with ARB, *Appl. Environ. Microbiol.*, 2006, **72**, 5069–5072.

58 S. Andrews, FastQC A Quality Control tool for High Throughput Sequence Data, https://www.bioinformatics.babraham.ac.uk/projects/fastqc/, accessed 16 September 2024.

59 A. V. Zimin, G. Marçais, D. Puiu, M. Roberts, S. L. Salzberg and J. A. Yorke, The MaSuRCA genome assembler, *Bioinformatics*, 2013, **29**, 2669–2677.

60 F. A. Simão, R. M. Waterhouse, P. Ioannidis, E. V. Kriventseva and E. M. Zdobnov, BUSCO: assessing genome assembly and annotation completeness with single-copy orthologs, *Bioinformatics*, 2015, **31**, 3210–3212.

61 A. Gurevich, V. Saveliev, N. Vyahhi and G. Tesler, QUAST: quality assessment tool for genome assemblies, *Bioinformatics*, 2013, **29**, 1072–1075.

62 T. Seemann, Prokka: rapid prokaryotic genome annotation, *Bioinformatics*, 2014, **30**, 2068–2069.

63 Y. Tanizawa, T. Fujisawa and Y. Nakamura, DFAST: a flexible prokaryotic genome annotation pipeline for faster genome publication, *Bioinformatics*, 2018, **34**, 1037–1039.

64 B. P. Alcock, W. Huynh, R. Chalil, K. W. Smith, A. R. Raphenya, M. A. Wlodarski, A. Edalatmand, A. Petkau, S. A. Syed, K. K. Tsang, S. J. C. Baker, M. Dave, M. C. McCarthy, K. M. Mukiri, J. A. Nasir, B. Golbon, H. Imtiaz, X. Jiang, K. Kaur, M. Kwong, Z. C. Liang, K. C. Niu, P. Shan, J. Y. J. Yang, K. L. Gray, G. R. Hoad, B. Jia, T. Bhando, L. A. Carfrae, M. A. Farha, S. French, R. Gordzevich, K. Rachwalski, M. M. Tu, E. Bordeleau, D. Dooley, E. Griffiths, H. L. Zubyk, E. D. Brown, F. Maguire, R. G. Beiko, W. W. L. Hsiao, F. S. L. Brinkman, G. Van Domselaar and A. G. McArthur, CARD 2023: expanded curation, support for machine learning, and resistome prediction at the Comprehensive Antibiotic Resistance Database, *Nucleic Acids Res.*, 2023, **51**, D690–D699.

65 S. Cosentino, M. Voldby Larsen, F. Møller Aarestrup and O. Lund, Correction: PathogenFinder - Distinguishing Friend from Foe Using Bacterial Whole Genome Sequence Data, *PLoS One*, 2013, **8**(12), DOI: 10.1371/annotation/b84e1af7-c127-45c3-be22-76abd977600f.

66 S. Cosentino, M. Voldby Larsen, F. Møller Aarestrup and O. Lund, PathogenFinder - Distinguishing Friend from Foe Using Bacterial Whole Genome Sequence Data, *PLoS One*, 2013, **8**, e77302.

© 2025 The Author(s). Published by the Royal Society of Chemistry

Environ. Sci.: Adv., 2025, **4**, 1444–1476 | **1473**

67 K. G. Joensen, F. Scheutz, O. Lund, H. Hasman, R. S. Kaas, E. M. Nielsen and F. M. Aarestrup, Real-Time Whole-Genome Sequencing for Routine Typing, Surveillance, and Outbreak Detection of Verotoxigenic *Escherichia coli*, *J. Clin. Microbiol.*, 2014, **52**, 1501–1510.

68 K. Blin, S. Shaw, H. E. Augustijn, Z. L. Reitz, F. Biermann, M. Alanjary, A. Fetter, B. R. Terlouw, W. W. Metcalf, E. J. N. Helfrich, G. P. van Wezel, M. H. Medema and T. Weber, antiSMASH 7.0: new and improved predictions for detection, regulation, chemical structures and visualisation, *Nucleic Acids Res.*, 2023, **51**, W46–W50.

69 M. H. K. Johansson, V. Bortolaia, S. Tansirichaiya, F. M. Aarestrup, A. P. Roberts and T. N. Petersen, Detection of mobile genetic elements associated with antibiotic resistance in *Salmonella enterica* using a newly developed web tool: MobileElementFinder, *J. Antimicrob. Chemother.*, 2021, **76**, 101–109.

70 R. Zallot, N. Oberg and J. A. Gerlt, The EFI Web Resource for Genomic Enzymology Tools: Leveraging Protein, Genome, and Metagenome Databases to Discover Novel Enzymes and Metabolic Pathways, *Biochemistry*, 2019, **58**, 4169–4182.

71 N. Oberg, R. Zallot and J. A. Gerlt, EFI-EST, EFI-GNT, and EFI-CGFP: Enzyme Function Initiative (EFI) Web Resource for Genomic Enzymology Tools, *J. Mol. Biol.*, 2023, **435**, 168018.

72 G. Su, J. H. Morris, B. Demchak and G. D. Bader, Biological Network Exploration with Cytoscape 3, *Curr. Protoc. Bioinf.*, 2014, **47**, 1–24.

73 Y. Xie, H. Li, X. Luo, H. Li, Q. Gao, L. Zhang, Y. Teng, Q. Zhao, Z. Zuo and J. Ren, IBS 2.0: an upgraded illustrator for the visualization of biological sequences, *Nucleic Acids Res.*, 2022, **50**, W420–W426.

74 S. Y. Wee and A. Z. Aris, Revisiting the "forever chemicals", PFOA and PFOS exposure in drinking water, *npj Clean Water*, 2023, **6**, 57.

75 Y. Wang and K. D. Good, Microplastics and PFAS air-water interaction and deposition, *Sci. Total Environ.*, 2024, **954**, 176247.

76 T. A. Bruton and D. L. Sedlak, Treatment of Aqueous Film-Forming Foam by Heat-Activated Persulfate Under Conditions Representative of In Situ Chemical Oxidation, *Environ. Sci. Technol.*, 2017, **51**, 13878–13885.

77 W. Cai, D. A. Navarro, J. Du, P. Srivastava, Z. Cao, G. Ying and R. S. Kookana, Effect of heavy metal co-contaminants on the sorption of thirteen anionic per- and poly-fluoroalkyl substances (PFAS) in soils, *Sci. Total Environ.*, 2023, **905**, 167188.

78 G. A. Zavarzin, Winogradsky and modern microbiology, *Microbiology*, 2006, **75**, 501–511.

79 V. Passet and S. Brisse, Description of *Klebsiella grimontii* sp. nov, *Int. J. Syst. Evol. Microbiol.*, 2018, **68**, 377–381.

80 C. A. Broberg, M. Palacios and V. L. Miller, *Klebsiella*: a long way to go towards understanding this enigmatic jet-setter, *F1000Prime Rep.*, 2014, **6**, 64, DOI: 10.12703/P6-64.

81 N. Barnich, M.-A. Bringer, L. Claret and A. Darfeuille-Michaud, Involvement of Lipoprotein NlpI in the Virulence of Adherent Invasive *Escherichia coli* Strain LF82 Isolated from a Patient with Crohn's Disease, *Infect. Immun.*, 2004, **72**, 2484–2493.

82 K. L. Stewart, A. M. Stewart and T. A. Bobik, Prokaryotic Organelles: Bacterial Microcompartments in *E. coli* and *Salmonella*, *EcoSal Plus*, 2020, **9**(1), DOI: 10.1128/ecosalplus.ESP-0025–2019.

83 B. Ferlez, M. Sutter and C. A. Kerfeld, Glycyl Radical Enzyme-Associated Microcompartments: Redox-Replete Bacterial Organelles, *mBio*, 2019, **10**, e02327.

84 C. A. Huffine, L. C. Wheeler, B. Wing and J. C. Cameron, Computational modeling and evolutionary implications of biochemical reactions in bacterial microcompartments, *Curr. Opin. Microbiol.*, 2022, **65**, 15–23.

85 T. I. Herring, T. N. Harris, C. Chowdhury, S. K. Mohanty and T. A. Bobik, A Bacterial Microcompartment Is Used for Choline Fermentation by *Escherichia coli* 536, *J. Bacteriol.*, 2018, **200**(10), e00764.

86 E. Jameson, T. Fu, I. R. Brown, K. Paszkiewicz, K. J. Purdy, S. Frank and Y. Chen, Anaerobic choline metabolism in microcompartments promotes growth and swarming of *Proteus mirabilis*, *Environ. Microbiol.*, 2016, **18**, 2886–2898.

87 G. Kalnins, J. Kuka, S. Grinberga, M. Makrecka-Kuka, E. Liepinsh, M. Dambrova and K. Tars, Structure and Function of CutC Choline Lyase from Human Microbiota Bacterium *Klebsiella pneumoniae*, *J. Biol. Chem.*, 2015, **290**, 21732–21740.

88 G. Kalnins, E.-E. Cesle, J. Jansons, J. Liepins, A. Filimonenko and K. Tars, Encapsulation mechanisms and structural studies of GRM2 bacterial microcompartment particles, *Nat. Commun.*, 2020, **11**, 388.

89 Y. Chen, Y. Liu, R. Zhou, X. Chen, C. Wang, X. Tan, L. Wang, R. Zheng, H. Zhang, W. Ling and H. Zhu, Associations of gut-flora-dependent metabolite trimethylamine-N-oxide, betaine and choline with non-alcoholic fatty liver disease in adults, *Sci. Rep.*, 2016, **6**, 19076.

90 M. Trøseid, T. Ueland, J. R. Hov, A. Svardal, I. Gregersen, C. P. Dahl, S. Aakhus, E. Gude, B. Bjørndal, B. Halvorsen, T. H. Karlsen, P. Aukrust, L. Gullestad, R. K. Berge and A. Yndestad, Microbiota-dependent metabolite trimethylamine-N-oxide is associated with disease severity and survival of patients with chronic heart failure, *J. Intern. Med.*, 2015, **277**, 717–726.

91 W. H. W. Tang, Z. Wang, B. S. Levison, R. A. Koeth, E. B. Britt, X. Fu, Y. Wu and S. L. Hazen, Intestinal Microbial Metabolism of Phosphatidylcholine and Cardiovascular Risk, *N. Engl. J. Med.*, 2013, **368**, 1575–1584.

92 W. H. W. Tang, Z. Wang, D. J. Kennedy, Y. Wu, J. A. Buffa, B. Agatisa-Boyle, X. S. Li, B. S. Levison and S. L. Hazen, Gut Microbiota-Dependent Trimethylamine *N*-Oxide (TMAO) Pathway Contributes to Both Development of Renal Insufficiency and Mortality Risk in Chronic Kidney Disease, *Circ. Res.*, 2015, **116**, 448–455.

93 W. H. W. Tang, Z. Wang, X. S. Li, Y. Fan, D. S. Li, Y. Wu and S. L. Hazen, Increased Trimethylamine N-Oxide Portends High Mortality Risk Independent of Glycemic Control in Patients with Type 2 Diabetes Mellitus, *Clin. Chem.*, 2017, **63**, 297–306.

94 P. Kaufmann, B. R. Duffus, B. Mitrova, C. Iobbi-Nivol, C. Teutloff, M. Nimtz, L. Jänsch, U. Wollenberger and S. Leimkühler, Modulating the Molybdenum Coordination Sphere of *Escherichia coli* Trimethylamine *N*-Oxide Reductase, *Biochemistry*, 2018, **57**, 1130–1143.

95 K. Nagórska, A. Ostrowski, K. Hinc, I. B. Holland and M. Obuchowski, Importance ofeps genes from *Bacillus subtilis* in biofilm formation and swarming, *J. Appl. Genet.*, 2010, **51**, 369–381.

96 D. J. Brenner, P. A. D. Grimont, A. G. Steigerwalt, G. R. Fanning, E. Ageron and C. F. Riddle, Classification of Citrobacteria by DNA Hybridization: Designation of *Citrobacter farmeri* sp. nov., *Citrobacter youngae* sp. nov., *Citrobacter braakii* sp. nov., *Citrobacter werkmanii* sp. nov., *Citrobacter sedlakii* sp. nov., and Three Unnamed *Citrobacter* Genomospecies, *Int. J. Syst. Bacteriol.*, 1993, **43**, 645–658.

97 H. Han, Z. Zhao, Y. Lin, B. Lin, H. Xu and B. Zheng, Co-Production of NDM-1 and OXA-10 β-Lactamase in *Citrobacter braakii* Strain Causing Urinary Tract Infection, *Infect. Drug Resist.*, 2022, **15**, 1127–1133.

98 A. Shnaiderman-Torban, S. Navon-Venezia, H. Baron, W. Abu-Ahmad, H. Arielly, G. Zizelski Valenci, I. Nissan, Y. Paitan and A. Steinman, Prevalence and Molecular Characterization of Extended-Spectrum β-Lactamase Producing Enterobacterales in Healthy Community Dogs in Israel, *Antibiotics*, 2022, **11**, 1069.

99 A. L. Colclough, I. Alav, E. E. Whittle, H. L. Pugh, E. M. Darby, S. W. Legood, H. E. McNeil and J. M. Blair, RND Efflux Pumps in Gram-Negative Bacteria; Regulation, Structure and Role in Antibiotic Resistance, *Future Microbiol.*, 2020, **15**, 143–157.

100 L. Hadchity, J. Houard, A. Lanois, A. Payelleville, F. Nassar, M. Gualtieri, A. Givaudan and Z. Abi Khattar, The AcrAB efflux pump confers self-resistance to stilbenes in *Photorhabdus laumondii*, *Res. Microbiol.*, 2023, **174**, 104081.

101 A. Pérez, M. Poza, A. Fernández, M. Del Carmen Fernández, S. Mallo, M. Merino, S. Rumbo-Feal, M. P. Cabral and G. Bou, Involvement of the AcrAB-TolC Efflux Pump in the Resistance, Fitness, and Virulence of *Enterobacter cloacae*, *Antimicrob. Agents Chemother.*, 2012, **56**, 2084–2090.

102 I. Johnston, L. J. Osborn, R. L. Markley, E. A. McManus, A. Kadam, K. B. Schultz, N. Nagajothi, P. P. Ahern, J. M. Brown and J. Claesen, Identification of essential genes for *Escherichia coli* aryl polyene biosynthesis and function in biofilm formation, *npj Biofilms Microbiomes*, 2021, **7**, 56.

103 F. Prestinaci, P. Pezzotti and A. Pantosti, Antimicrobial resistance: a global multifaceted phenomenon, *Pathog. Global Health*, 2015, **109**, 309–318.

104 M. Irfan, A. Almotiri and Z. A. AlZeyadi, Antimicrobial Resistance and Its Drivers—A Review, *Antibiotics*, 2022, **11**, 1362.

105 V. M. D'Costa, C. E. King, L. Kalan, M. Morar, W. W. L. Sung, C. Schwarz, D. Froese, G. Zazula, F. Calmels, R. Debruyne, G. B. Golding, H. N. Poinar and G. D. Wright, Antibiotic resistance is ancient, *Nature*, 2011, **477**, 457–461.

106 K. Hwengwere, H. Paramel Nair, K. A. Hughes, L. S. Peck, M. S. Clark and C. A. Walker, Antimicrobial resistance in Antarctica: is it still a pristine environment?, *Microbiome*, 2022, **10**, 71.

107 L. C. Scott, N. Lee and T. G. Aw, Antibiotic Resistance in Minimally Human-Impacted Environments, *Int. J. Environ. Res. Public Health*, 2020, **17**, 3939.

108 C. Ejikeugwu, O. Nworie, M. Saki, H. O. M. Al-Dahmoshi, N. S. K. Al-Khafaji, C. Ezeador, E. Nwakaeze, P. Eze, E. Oni, C. Obi, I. Iroha, C. Esimone and M. U. Adikwu, Metallo-β-lactamase and AmpC genes in *Escherichia coli, Klebsiella pneumoniae, and Pseudomonas aeruginosa* isolates from abattoir and poultry origin in Nigeria, *BMC Microbiol.*, 2021, **21**, 124.

109 M. Saki, A. F. Sheikh, S. Seyed-Mohammadi, A. A. Z. Dezfuli, M. Shahin, M. Tabasi, H. Veisi, R. Keshavarzi and P. Khani, Publisher Correction: Occurrence of plasmid-mediated quinolone resistance genes in *Pseudomonas aeruginosa* strains isolated from clinical specimens in southwest Iran: a multicentral study, *Sci. Rep.*, 2022, **12**, 3817.

110 F. Abbasian, R. Lockington, M. Mallavarapu and R. Naidu, A pyrosequencing-based analysis of microbial diversity governed by ecological conditions in the Winogradsky column, *World J. Microbiol. Biotechnol.*, 2015, **31**, 1115–1126.

111 R. Sridharan, M. Vetriselvan, V. G. Krishnaswamy, S. Jansi R, H. Rishin, T. Kumar D and G. P. Doss C, Integrated approach in LDPE degradation – An application using Winogradsky column, computational modeling, and pathway prediction, *J. Hazard. Mater.*, 2021, **412**, 125336.

112 S. Brisse, F. Grimont and P. A. D. Grimont, in *The Prokaryotes*, ed. M. Dworkin, S. Falkow, E. Rosenberg, K.-H. Schleifer and E. Stackebrandt, Springer New York, New York, NY, 2006, pp. , pp. 159–196.

113 M. K. Paczosa and J. Mecsas, *Klebsiella pneumoniae*: Going on the Offense with a Strong Defense, *Microbiol. Mol. Biol. Rev.*, 2016, **80**, 629–661.

114 T. I. Doran, The Role of *Citrobacter* in Clinical Disease of Children: Review, *Clin. Infect. Dis.*, 1999, **28**, 384–394.

115 G. Samonis, D. E. Karageorgopoulos, D. P. Kofteridis, D. K. Matthaiou, V. Sidiropoulou, S. Maraki and M. E. Falagas, *Citrobacter* infections in a general hospital: characteristics and outcomes, *Eur. J. Clin. Microbiol. Infect. Dis.*, 2009, **28**, 61–68.

116 A. Nawaz, F. Mubeen, Z. U. Qamar, M. U. Marghoob, S. Aziz and H. Gross, Draft Genome Sequence of the Halophilic Strain *Citrobacter braakii* AN-PRR1, Isolated from Rhizospheric Soil of Rice (Oryza sativa L.) from Pakistan, *Microbiol. Resour. Announce.*, 2021, **10**, e00787.

117 R. Gupta, S. J. Rauf, S. Singh, J. Smith and M. L. Agraharkar, Sepsis in a Renal Transplant Recipient due to *Citrobacter braakii*, *South. Med. J.*, 2003, **96**, 796–798.

118 E. Tollkuci and R. Myers, *Citrobacter braakii* CLABSI in a hematopoietic stem cell transplant patient, *J. Oncol. Pharm. Pract.*, 2021, **27**, 1792–1794.

© 2025 The Author(s). Published by the Royal Society of Chemistry

Environ. Sci.: Adv., 2025, **4**, 1444–1476 | **1475**

119 V. Prasanna, R. Rana, D. K. Daunaria and N. B. Patel, Bacteremia due to carbapenem-resistant *Citrobacter braakii*, *J. Fam. Med. Prim. Care*, 2022, **11**, 3395.

120 M. O. A. Sommer, G. Dantas and G. M. Church, Functional Characterization of the Antibiotic Resistance Reservoir in the Human Microflora, *Science*, 2009, **325**, 1128–1131.

121 S. P. Brown, D. M. Cornforth and N. Mideo, Evolution of virulence in opportunistic pathogens: generalism, plasticity, and control, *Trends Microbiol.*, 2012, **20**, 336–342.

122 A. Salyers, A. Gupta and Y. Wang, Human intestinal bacteria as reservoirs for antibiotic resistance genes, *Trends Microbiol.*, 2004, **12**, 412–416.

123 C. J. H. Von Wintersdorff, J. Penders, J. M. Van Niekerk, N. D. Mills, S. Majumder, L. B. Van Alphen, P. H. M. Savelkoul and P. F. G. Wolffs, Dissemination of Antimicrobial Resistance in Microbial Ecosystems through Horizontal Gene Transfer, *Front. Microbiol.*, 2016, **7**, 173.

124 S. Bhatt and S. Chatterjee, Fluoroquinolone antibiotics: Occurrence, mode of action, resistance, environmental detection, and remediation – A comprehensive review, *Environ. Pollut.*, 2022, **315**, 120440.

125 L. S. Redgrave, S. B. Sutton, M. A. Webber and L. J. V. Piddock, Fluoroquinolone resistance: mechanisms, impact on bacteria, and role in evolutionary success, *Trends Microbiol.*, 2014, **22**, 438–445.

126 O. Lomovskaya, K. Lewis and A. Matin, EmrR is a negative regulator of the *Escherichia coli* multidrug resistance pump EmrAB, *J. Bacteriol.*, 1995, **177**, 2328–2334.

127 N. Yousefian, A. Ornik-Cha, S. Poussard, M. Decossas, M. Berbon, L. Daury, J.-C. Taveau, J.-W. Dupuy, S. Đorđević-Marquardt, O. Lambert and K. M. Pos, Structural characterization of the EmrAB-TolC efflux complex from *E. coli*, *Biochim. Biophys. Acta, Biomembr.*, 2021, **1863**, 183488.

128 J. Li, H. Zhang, J. Ning, A. Sajid, G. Cheng, Z. Yuan and H. Hao, The nature and epidemiology of OqxAB, a multidrug efflux pump, *Antimicrob. Resist. Infect. Control*, 2019, **8**, 44.

129 L. H. Hansen, L. B. Jensen, H. I. Sørensen and S. J. Sørensen, Substrate specificity of the OqxAB multidrug resistance pump in *Escherichia coli* and

selected enteric bacteria, *J. Antimicrob. Chemother.*, 2007, **60**, 145–147.

130 X. He, F. Lu, F. Yuan, D. Jiang, P. Zhao, J. Zhu, H. Cheng, J. Cao and G. Lu, Biofilm Formation Caused by Clinical *Acinetobacter baumannii* Isolates Is Associated with Overexpression of the AdeFGH Efflux Pump, *Antimicrob. Agents Chemother.*, 2015, **59**, 4817–4825.

131 S. Coyne, N. Rosenfeld, T. Lambert, P. Courvalin and B. Périchon, Overexpression of Resistance-Nodulation-Cell Division Pump AdeFGH Confers Multidrug Resistance in *Acinetobacter baumannii*, *Antimicrob. Agents Chemother.*, 2010, **54**, 4389–4393.

132 V. B. Srinivasan and G. Rajamohan, KpnEF, a New Member of the *Klebsiella pneumoniae* Cell Envelope Stress Response Regulon, Is an SMR-Type Efflux Pump Involved in Broad-Spectrum Antimicrobial Resistance, *Antimicrob. Agents Chemother.*, 2013, **57**, 4449–4462.

133 V. B. Srinivasan, B. B. Singh, N. Priyadarshi, N. K. Chauhan and G. Rajamohan, Role of Novel Multidrug Efflux Pump Involved in Drug Resistance in *Klebsiella pneumoniae*, *PLoS One*, 2014, **9**, e96288.

134 Z. Xu, J. Xiong, C. Li, S. Hu, Z. Li, Y. Ma, S. Li, B. Huang, X. Ren and X. Pan, Environmental concentrations of per/polyfluoroalkyl substances promote the conjugative transfer of antibiotic resistance genes, *Chem. Eng. J.*, 2024, **498**, 155500.

135 V.-A. Thai, V. D. Dang, N. T. Thuy, B. Pandit, T.-K.-Q. Vo and A. P. Khedulkar, Fluoroquinolones: Fate, effects on the environment and selected removal methods, *J. Cleaner Prod.*, 2023, **418**, 137762.

136 N. R. Johnston and S. A. Strobel, Principles of fluoride toxicity and the cellular response: a review, *Arch. Toxicol.*, 2020, **94**, 1051–1069.

137 O. Barbier, L. Arreola-Mendoza and L. M. Del Razo, Molecular mechanisms of fluoride toxicity, *Chem.-Biol. Interact.*, 2010, **188**, 319–333.

138 Y. Zhao, X. Liu, C. Liang, T. Pei, M. Guo, J. Wang and J. Zhang, α-Lipoic Acid Alleviated Fluoride-Induced Hepatocyte Injury via Inhibiting Ferroptosis, *J. Agric. Food Chem.*, 2022, **70**, 15962–15971.

139 E. Terzioğlu, M. Arslan, B. G. Balaban and Z. P. Çakar, Microbial silver resistance mechanisms: recent developments, *World J. Microbiol. Biotechnol.*, 2022, **38**, 158.